

An Updated Look at Binary Characteristics of Massive Stars in the Cygnus OB2 Association

Daniel C. Kiminki^{1,2} & Henry A. Kobulnicky¹

ABSTRACT

This work provides a statistical analysis of the massive star binary characteristics in the Cygnus OB2 Association using radial velocity information of 114 B3–O3 primary stars and orbital properties for the 24 known binaries. We compare these data to a series of Monte Carlo simulations to infer the intrinsic binary fraction and distributions of mass ratios, periods, and eccentricities. We model the distribution of mass ratio, log-period, and eccentricity as power-laws and find best fitting indices of $\alpha = 0.1 \pm 0.5$, $\beta = 0.2 \pm 0.4$, and $\gamma = -0.6 \pm 0.3$ respectively. These distributions indicate a preference for massive companions, short periods, and low eccentricities. Our analysis indicates that the binary fraction of the cluster is $44 \pm 8\%$ if all binary systems are (artificially) assumed to have $P < 1000$ days; if the power-law period distribution is extrapolated to 10^4 years, a plausible upper limit for bound systems, the binary fraction is $\sim 90 \pm 10\%$. Of these binary (or higher order) systems, $\sim 45\%$ will have companions close enough to interact during pre- or post-main-sequence evolution (semi-major axis $\lesssim 4.7$ AU). The period distribution for $P < 27$ d is not well reproduced by any single power-law owing to an excess of systems with periods around 3–5 days (0.08–0.31 AU) and a relative shortage of systems with periods around 7–14 days (0.14–0.62 AU). We explore the idea that these longer-period systems evolved to produce the observed excess of short-period systems. The best fitting binary parameters imply that secondaries generate, on average, $\sim 16\%$ of the V-band light in young massive populations. This means that photometrically based distance measurements for young massive clusters & associations will be systematically low by $\sim 8\%$ (0.16 mag in the distance modulus) if the luminous contributions of unresolved secondaries are not taken into account.

Subject headings: techniques: radial velocities — binaries: general — (stars:) binaries: spectroscopic — (stars:) binaries: (*including multiple*) close — stars: early-type — stars: kinematics — surveys

¹Dept. of Physics & Astronomy, University of Wyoming, Laramie, WY 82070

²Dept. of Astronomy, University of Arizona, Tucson, AZ 85721

1. Introduction

In clusters containing high concentrations of massive stars (B3 and earlier), binary and multiple systems provide a virtual cornucopia of information about the massive stars and the nature of their formation process. In addition to the frequency at which they occur, we may examine the distribution of several quasi-preserved orbital parameters (e.g., period, mass ratio, and eccentricity) and gain insight into many open questions surrounding massive stars, such as whether they form in isolation or as part of a competing menagerie of protostars (for a review see Zinnecker & Yorke 2007). Other issues include whether there exists an evolutionary link between massive binary systems and type Ib/c supernovae (Kobulnicky & Fryer 2007; Podsiadlowski et al. 1992), whether there is a correlation between the massive binary fraction and the stellar density of the parent cluster (Sana et al. 2008; Garcia & Mermilliod 2001), whether massive binaries are responsible for the runaway OB stars (Blaauw 1961), and what role these stars play in short and long γ -ray bursts (Fryer et al. 1999). Previous and current endeavors to characterize the binary properties of massive stars include the galactic O-star binary study of Garmany et al. (1980), the Galactic O-star speckle survey of Maíz et al (2004), the multi-cluster O-star binary statistical analysis of Garcia & Mermilliod (2001), the VLT-FLAMES studies of the Large and Small Magellanic Clouds (Evans et al. 2006), the lucky imaging O-star study of Maíz (2010), the adaptive optics O-star studies of Turner et al. (2008), Duchêne (2001), and Sana et al. (2010), the HST Fine Guidance Sensor survey of Cyg OB2 by Caballero-Nieves et al. (2011), and the individual open cluster binary spectroscopic studies of Sana et al. (2009), Mahy et al. (2009), Sana et al. (2008), Rauw & De Becker (2004), De Becker et al. (2006), Hillwig (2006), and Mermilliod (1995). These studies have found a broad range of binary fractions (0–63%; Sana & Evans 2011) and widely varying characterizations of the intrinsic orbital parameter distributions, including single power law descriptions with various indices and multiple-component descriptions requiring many free parameters. Reasons for the diverse, and seemingly incompatible, results in the literature stem from the varying methodologies and biases inherent in the surveys themselves. The majority of massive binary surveys in the literature include either a small sample of O stars within a given cluster or larger samples assembled from multiple smaller surveys encompassing different clusters & associations (e.g., Garmany et al. 1980; Gies 1987; Evans et al. 2006; Mason et al. 2009). The larger surveys have the advantage of better statistics, but the smaller surveys have the advantage of a more homogeneous sample (same formation environment and similar ages).

The Cyg OB2 radial velocity survey (Kiminki et al. 2007, Kiminki et al. 2008, Kiminki et al. 2009, Kiminki et al. 2010, and Kobulnicky et al. 2012, in prep; Papers I, II, III, IV, & VI), takes advantage of both a large and homogeneous sample of OB stars (114 massive stars) with radial velocity coverage of up to 12 years to probe the binary characteristics of massive

stars. Kobulnicky & Fryer (2007, KF07) analyzed the Cyg OB2 radial velocity data from 1999–2005 and compared the raw velocities with the expectations of Monte Carlo simulations over a range of mass ratio and orbital separation distributions and at varying binary fractions.¹ They find that the likely binary fraction of OB stars within Cyg OB2 is greater than 70% for an Öpik (1924) period distribution (i.e., log-flat) and mass ratio distribution best characterized by a power-law slope of $\alpha = -0.6$ to 1.0 (depending on the choice of binary fraction). Though KF07 are very thorough in addressing different possible distribution scenarios (a second “twin” population, a Hogeveen 1992 distribution, a Miller & Scalo 1979 secondary mass distribution, etc), they are forced to make certain simplifying assumptions in their code based on the limited binary information available. A few of the more significant assumptions are circular orbits, treating all higher order systems as binaries rather than triples, quadruples, etc, and finally, that all velocity variation stems from orbital dynamics rather than stellar atmosphere line profile variations, which may be present in massive stars. Assuming circular orbits can cause an underestimation of the binary fraction because fewer circular binaries need to be generated to simulate the seemingly singular eccentric systems that exist in the cluster. With regard to the next assumption, treating (difficult-to-detect) triple and quadruple systems as binaries still yields a meaningful estimate of the binary fraction of the cluster, as long as this term is understood to include possible higher order systems. Lastly, the assumption that all velocity variation stems from orbital dynamics can lead to an overestimation of the binary fraction or an overestimation of number of massive companions, but this is an unavoidable limitation to the KF07 analysis.

We present here a follow-up to the initial results of Papers I, II, III, IV, & VI, and the earlier analysis of KF07. We use the results of nearly 12 years of spectroscopic observations obtained on 114 massive stars in the Cyg OB2 Association to model the observed mass ratio, orbital period, and eccentricity distributions composed from the orbital information of 22 close massive binaries in the cluster. We make use of all published close binary information for the cluster, both photometric and spectroscopic, including single-lined spectroscopic binaries (SB1s), double-lined spectroscopic binaries (SB2s), and eclipsing binaries. We also use the radial velocity information of 110 OB stars from our original sample from Massey & Thompson (1991) to infer the binary fraction of the cluster. Additionally, we examine, in more detail, an apparent excess of binary systems with periods between 3 and 5 days that have been observed in Cyg OB2 (Kiminki et al. 2009) and other clusters (NGC 6231; Sana et al. 2008). The current work provides an analysis using the largest sample of massive

¹We define the massive star binary fraction to mean the number of systems with two (or more) components divided by the total number systems containing at least one massive star. We caution the reader that other definitions exist in the literature.

stars and close massive binary systems ever compiled for a group of stars with a shared history.

Section 2 reviews the data used in this work. Section 3 summarizes the method employed in this work to model the orbital period, eccentricity, and mass ratio distributions using a Monte Carlo approach. Section 4 presents the results of the Monte Carlo simulations and discusses the most probable intrinsic orbital parameter distributions and the probable binary fraction of massive stars within the cluster. Discussion in Section 5 explores possible physical origins for the observed orbital distributions and summarizes results that may inform models of close binaries as progenitors to supernova and γ -ray bursts. Finally, Section 6 summarizes the survey findings.

2. The Data

We obtained radial velocities for a total of 146 OB stars over 12 years. These 146 (given in Table 1 of Paper I) were chosen from the *UBV* photometric and spectroscopic survey of Cyg OB2 by Massey & Thompson (1991). Nearly half of the stars were previously identified as an OB-type and the other half had colors consistent with classification of B3 or earlier. In this work, we utilize 110 of the 146 Massey & Thompson (1991) stars, termed the “unbiased” sample because they were selected on a “binary-blind” basis (i.e., no previous evidence of a companion). The objects in the “unbiased” sample average 14 observations over 1999–2011 with a mean velocity uncertainty of 9.7 km s^{-1} . Stars were removed from the original sample for having fewer than three observations at sufficiently high S/N needed to obtain reliable velocities (i.e., $S/N < 30$ where velocity uncertainties are $> 40 \text{ km s}^{-1}$) and for having spectral types later than B3. Additionally, we include the published orbital information for four systems not in our original sample, but likely members of Cyg OB2: Schulte 5 from Schulte (1958), A36, A45, and B17 from Comerón et al. (2002). This constitutes 114 OB stars and is designated the “complete” sample. The primary components in the “complete” sample have spectral types that range from B3V (e.g., MT298) to O3If (e.g., MT457) and masses that range from $7.6 M_{\odot}$ to $80 M_{\odot}$ (initial masses were interpolated from the stellar evolutionary models of Lejeune & Schaerer 2001) with a mean mass of $\sim 20 M_{\odot}$ and mean temperature class of B0 (71 B3–B0 stars and 43 O9.5–O3 stars).

There are fewer stars than included in KF07 (who included stars from Table 5 of Paper I) owing to removal of seven stars having temperature classes later than B3 (MT196, MT239, MT271, MT453, MT493, MT576, and MT641), 13 stars having fewer than three observations with sufficient S/N (MT238, MT343, MT435, MT477, MT490, MT492, MT493, MT509, MT568, MT621, MT645, MT650, and MT712), and one star that is a newly turned-on Be

star (MT213). Additionally, ten stars not included in the analysis of KF07 but included here are Schulte 3, Schulte 73, MT005, MT179, MT186, MT222, MT241, MT267, MT421, and MT426. These ten stars were excluded from the earlier work because they had fewer than three observations prior to 2007. In total, this survey has produced full or partial orbital solutions for 19 binary systems. Combined with the other published data, there are 24 known OB binary systems in Cyg OB2. The locations of the first 20 are shown by the open circles in Figure 16 of Paper IV and listed in Table 6 therein. The remaining 4 are presented in Paper VI.

3. Current Approach to Monte Carlo Analysis

In keeping with prior works, we characterize the orbital parameter distributions as single power-laws. The mass ratio distribution is represented by $f(q) \propto q^\alpha$ (where $q = M_2/M_1$) over a range of q_{MIN} to 1, the period distribution is represented by $f(\log P) \propto (\log P)^\beta$ over a range of periods from P_{MIN} to P_{MAX} days, and the eccentricity distribution is represented by $f(e) \propto e^\gamma$ over a range of e_{MIN} to e_{MAX} . In the current approach, we constrain the indices, α , β , γ , by comparing the 12 years of radial velocity data, in addition to measured mass ratios, orbital periods, and eccentricities for the 22 binaries in Cyg OB2 with periods under 30 days, to Monte Carlo-generated binary populations. For the standard application of the Monte Carlo (MC) code, we adopt $q_{MIN} = 0.005$ (roughly representing the mass ratio of a B3V + M8V system; Drilling & Landolt 2000), $P_{MIN} = 1$ day, $P_{MAX} = 1000$ days, $e_{MIN} = 0.0001$, and $e_{MAX} = 0.9$. The period upper limit is chosen based on our observing campaign time span of a few thousand days. The eccentricity upper limit is chosen based roughly on where an orbital system becomes unbound. We show later that our results are not sensitive to the exact choices for these upper and lower bounds, the main exception being that the inferred binary fraction does depend on the choice of P_{MAX} .

We created synthetic binary populations using Monte Carlo (MC) methods by randomly drawing periods, mass ratios, and eccentricities from power-law distributions with indices ranging from -2 to 2 in increments of 0.1, with binary fractions ranging from 20%–100% in increments of 5%. The MC code then generates a 4-dimensional parameter space composed of $41 \times 41 \times 41 \times 17 = 1,171,657$ distinct “families” that are described by unique combinations of each parameter. During each iteration, radial velocities are calculated for a group of 110/114 synthetic stars whose primary masses are determined from the adopted values for Cyg OB2 primaries. The number of synthetic velocities for each system is determined by the actual number of observations for each given star in the survey. The code samples the synthetic velocity curve at intervals corresponding to the actual observing cadence for that star. If the

system is, at random, designated a binary, a mass ratio, eccentricity, and period are drawn from the power-law distributions characterized by the family currently being examined. An inclination is randomly drawn from a probability distribution described by $\sin(i)$ over an interval of 0 to $\pi/2$, representing a random orientation on the unit sphere (Law et al. 2009). The orbital phase and angle of periastron are randomly drawn from uniform distributions over their allowed values (i.e., $0-2\pi$). The code adds Gaussian noise to each simulated radial velocity, where the magnitude of the noise is set by the observational uncertainty from the actual observations of the selected star. For example, when a system representing MT720 is simulated, a primary mass of $17.5 M_{\odot}$ is used and 32 radial velocities are calculated using the dates and errors listed in Table 1. Finally, the code produces 300 realizations of each family, designated a “generation”. We compare the average properties of each generation to the Cyg OB2 data.

We constrain the binary fraction by comparing the χ^2 probability density function (PDF) for the simulated radial velocities to that of the unbiased sample of Cyg OB2 stars. We use the same method described in Paper I, where the probability corresponds to the likelihood that the χ^2 for each star’s radial velocity measurements, as considered around the weighted mean velocity, would be exceeded by chance given $\nu = N_{OBS} - 1$ degrees of freedom. We compare the observed χ^2 PDF to simulated ones for each generation using a 2-sided Kolgorov-Smirnov (K–S) test. In our tests of the code, we were able to recover the binary fraction of a simulated dataset to within $\pm 5\%$.

In order to compare the Monte Carlo distributions of q , P , and e with the observed ones, it was necessary to apply a series of filters to the synthetic data to remove all binary systems with orbital solutions undetectable by this survey (i.e., the systems are designated “single” and the orbital parameters are not included in the final distributions). We first eliminate all synthetic systems have χ^2 probabilities $>5\%$; such systems either have large errors, few measurements, and/or small velocity amplitudes that preclude full orbital solutions. The next filter removes all synthetic systems that have a semi-amplitudes $K_{MIN} < 15 \text{ km s}^{-1}$, the minimum semi-amplitude for which we can derive a complete orbital solution given typical velocity uncertainties. In exceptional cases where the stellar lines are narrow, we are able to do better. For example, MT174, with $K_1 = 9 \text{ km s}^{-1}$ (Paper VI), has the smallest velocity semi-amplitude yet measured in the survey. Finally, we retain only systems that have periods within the 1.5–26.5 day range covered by the 19 systems with orbital solutions where our survey is highly complete (see Section 4.1). The final mean extracted synthetic orbital parameter distributions for each generation are then compared to the observed ones using 2-sided K–S tests. The final best-fit combination of α , β , γ is determined by product of the resultant individual K–S probabilities for each of the three parameter distributions.

In our testing of the code, we produced a series of simulated datasets (i.e., orbital parameter distributions and ephemerides), similar to the Cyg OB2 dataset, covering a large range of possible α , β , and γ combinations and binary fractions. The power-law indices ranged from -2.5 to 2.5 (and the MC code search grid was increased accordingly) and binary fractions ranged from 20% (the absolute minimum binary fraction of the Cyg OB2 sample based on current observations) to 100%. The simulated datasets were constructed using the observation cadences, velocity uncertainties, and primary masses from the Cyg OB2 data. The code was able to recover the original distribution indices to within ± 0.3 rms and the original binary fraction to within 5% rms. The magnitude of the uncertainty on each index is limited by the current sample size of $N=22$ systems having orbital solutions. The uncertainty on the binary fraction is limited by the mean number of observations per object and the mean observational uncertainty.

3.1. Limitations in the Code, Dataset, and Knowledge of Cyg OB2

While our current approach explores a larger parameter space than KF07, incorporates eccentric orbits, and utilizes the information of 22 close massive binary systems in addition to the radial velocity information of 12 years of spectroscopic observations, there are still several limitations stemming from our modeling approach, our dataset, and our current knowledge of Cyg OB2.

Limitations owing to our modeling approach: As in KF07, we still consider all velocity variation as stemming from orbital dynamics rather than atmospheric phenomena such as pulsations. Clark et al. (2010) show that pulsations in evolved early-type stars can significantly affect radial velocity measurements, meaning that this effect may add scatter to radial velocity measurements in roughly one-quarter of our sample. We also still treat higher order systems as binaries. At present, we know of three triple or higher order systems, Cyg OB2 No.5, Cyg OB2 No.8, and MT429 (see references in Table 6 of Paper IV). In addition, we limit characterization of each orbital parameter distribution to a single power-law, an assumption that may not hold.

Limitations owing to the dataset: As mentioned, the Cyg OB2 radial velocity survey probes binary systems with periods ranging from one day to a few thousand days, meaning we are not sensitive to extremely close (and extremely rare) systems with $P < 1$ d. Therefore, the MC code only draws from period distributions with periods ranging 1 to 1000 days. Additionally, the vast majority of spectroscopic observations were obtained June through November when Cygnus is visible to northern latitudes. This, coupled with typical velocity uncertainties of 9.7 km s^{-1} , reduces our sensitivity to long period, high eccentricity systems

(i.e., systems that may pass through periastron and exhibit their largest velocity variation during an unobservable period), systems with extreme mass ratios, and systems with small inclination angles. Even though we have detected and computed solutions for systems with semi-amplitudes as small as 9 km s^{-1} (Paper VI), we attempt to circumvent these limitations by designating systems in the code with semi-amplitudes smaller than 15 km s^{-1} as “single”.

Another limitation comes in the form of not being able to detect unresolved SB2s. For systems exhibiting highly blended line profiles (even at quadrature), such as long period binaries with mass and luminosity ratios near unity, radial velocity variations of the blended line profile will be small and possibly undetectable at the resolution of the spectra in this survey, thereby being designated as “single” by the code. Sana et al. (2009) discuss this effect in their analysis of the massive star binary fraction of NGC 6611 and conclude that the effect is minimal (affecting their modeling of the binary fraction by only a few percent). Additionally, there is also a negligible bias toward detecting short-period, high-mass-ratio systems that show up as SB2s as it only takes one observation at quadrature to determine that the system warrants follow-up. These systems, however, have large velocity separations (i.e., large semi-amplitudes) and will get flagged as a “binary” by the code with only a few observations.

Limitations owing to incomplete knowledge of Cyg OB2: A few studies have shown that Cyg OB2 may be contaminated by an older population of stars, meaning that evolutionary effects may be present (e.g., Wright et al. 2010; Drew et al. 2008; Comerón et al. 2008). However, Comerón et al. (2008) point out that the field star contamination is likely composed of F to late B stars at a radius of 1 degree. This exceeds the radial extent of the region examined in this study and concerns stars of a later type than are included here. On the other hand, some doubt remains in the membership of the 114 OB stars included in this work as recent findings by Stroud et al. (2010) and Linder et al. (2009) provide conflicting distance estimates to Cyg OB2 based on their complete orbital solutions calculated for the eclipsing SB2s, Cyg OB2 No.5 ($\sim 1 \text{ kpc}$) and B17 ($1.5\text{--}1.8 \text{ kpc}$) respectively. We maintain that the contamination is minor, if it exists, owing to the localized region we examine, but even the removal of a few periods or mass ratios could influence the distributions we observe at present. Similar to this is the assumption that the members of Cyg OB2 have a common age. It has been suggested that even within the core region of Cyg OB2, there has been more than one epoch of star formation (Wright et al. 2010). There are no clear predictions for how a population of close binaries should evolve over the 1–5 Myr lifetime of most massive stars in young clusters, so we have no way to model such effects or even know if they are important.

4. Results of the Monte Carlo Analysis

We use the Monte Carlo code in conjunction with the “complete” sample of Cyg OB2 data to infer the underlying distribution of orbital parameters, that is, α , β , γ . The orbital parameter information (but not ephemerides) for Schulte 9 and MT070 are excluded given their much longer periods. In order to address the binary fraction, however, we use the data of the “unbiased” sample. Ultimately, we find that the orbital parameter indices and binary fraction are essentially identical for both the “unbiased” and “complete” samples.

4.1. Period Distribution

Binary surveys that examine the orbital period distribution probe widely varying ranges in period/separation and stellar mass, and they find widely varying characterizations of its functional form. For solar-type stars with periods from 1–10,000+ days, Duquennoy & Mayor (1991) find a log-normal distribution. Among massive stars, most studies find a uniform distribution in log space ($\beta = 0$), sometimes known as an Öpik (1924) distribution. For example, Garmany et al. (1980) find $\beta \sim 0$ for a large number of Galactic O-star binaries in the northern hemisphere. Kouwenhoven et al. (2007) also find an Öpik’s distribution for a survey of visual and spectroscopic binaries in Sco OB2 composed of A- and B-type primaries (for $0.7 \text{ days} \leq P \leq 3 \times 10^8 \text{ days}$). Zinnecker & Yorke (2007) speculate that rather than a simple power-law distribution for O-star binaries, there may be a concentration of systems having periods between 2 and 5 days. The O-star binaries of NGC 6231 show this trend (Sana et al. 2008). However, Sana & Evans (2011) conclude that a broken Öpik distribution provides a better description of the period distribution for spectroscopic O-binaries in nearby clusters, where the broken distribution could better explain the higher concentration of systems with periods less than 10 days.

The observed orbital period, eccentricity, and mass ratio distributions for the 22 known close massive binaries in Cyg OB2 are shown in Figure 1. The orbital period and mass ratio distributions from Garmany et al. (1980) are also shown and represented by the dotted lines in the upper and lower panels, respectively. The Cyg OB2 and Garmany et al. (1980) period distributions show a concentration between 3 and 5 days (with a peak around 4–5 days for Cyg OB2). A possible explanation for such a concentration might be observational bias owing to the average observing run lasting a few days to a week. Three systems in Cyg OB2 with periods between 3 and 5 days originate from other studies (MT421, MT429, and B17) where this may be the case. However, the remaining five systems in this period range originate from our study which has a time coverage of up to 12 years and individual observing run durations of 1–3 weeks. This allows for a sensitivity to orbital periods up to 25 days without

appreciable bias. This abundance of 3–5 day systems is not limited to the SB2s having the largest mass ratios either. Three of the nine SB1s in Cyg OB2 also have periods that are in the 4–5 days range. This is illustrated in Figure 2, which shows eccentricity versus orbital period (upper panel) and mass-ratio (lower panel) versus orbital period. The SB1s and SB2s are the open and filled circles respectively, and the asterisks represent the orbital periods and eccentricities for the massive star binaries (primaries of type B3 and earlier) in the Ninth Spectroscopic Binary Catalog (Pourbaix et al. 2004). One can easily see the concentration of points around 3–5 days and a peculiar shortage of systems with periods from 7–14 days in the Cyg OB2 data. An initial hypothesis for this shortage of points might be that completeness plays a role. However, with multiple studies with varying observing cadences contributing to the catalog of binaries in Cyg OB2, we maintain that a more likely observation would be to see a continually diminishing number of binary detections with increasing period as completeness declines. Given the existence of this excess in periods around 3–5 days, we caution that a simple power-law may be insufficient to describe the distribution of orbital periods for early-type stars in this cluster.

In Figure 3, we show the results from the Monte Carlo analysis of the 22 close OB binaries in the “complete” sample. The four panels display the 1σ (68.3%), 2σ (95.4%), and 3σ (99.7%) contours relative to the maximum for the average probability of a generation as a function of two parameters for fixed best-fit values of the remaining two parameters. For example, the upper left panel shows the average probability as a function of α and γ for fixed best-fit values of β (0.2) and $B.F.$ (45%). The upper right panel similarly shows the average probability as a function of β and γ for fixed best-fit values of α (-0.1) and $B.F.$ (45%). The cross in each panel marks the location of the best fit for each parameter (i.e., the maximum of the average probability). We find that the period distribution is confined at the 1σ level to $-0.3 < \beta < 0.5$, with a best fit of $\beta = 0.2 \pm 0.4$. This points to a nearly log-flat distribution, consistent with Öpik’s Law (Öpik 1924), consistent with the previous O-star findings of Garmany et al. (1980), Kouwenhoven et al. (2007), Sana & Evans (2011), and KF07. Figure 4 shows the cumulative period distribution of the Cyg OB2 data (diamonds) and the best fit cumulative period distribution from the MC code (solid curve). The hump in the distribution at $\log(P) \sim 0.65$ or $P \sim 4.5$ days greatly influences the fit shown, and it is clear that a power-law of $\beta = 0$ might be a better fit if this hump were not present or less pronounced. Indeed, no single power-law provides a good fit to the cumulative period distribution. We address the peculiar nature of the period distribution in Section 5.

Figure 5 shows the survey completeness as a function of orbital period for the best-fitting power-law indices. We use the MC code to estimate the survey completeness by tallying the fraction of synthetic systems deemed detectable in our survey given the time sampling and velocity semi-amplitude limit of $K_{MIN} = 15 \text{ km s}^{-1}$. The survey is 88%

complete at $P = 10$ days and $\gtrsim 83\%$ complete at $P = 30$ days. Our completeness analysis implies that, given 14 detected binaries with periods $P < 10$ days, there are an additional 1–2 undetected binary systems in this range. Statistically, the Monte Carlo code shows that all of these would be undetectable by the survey because they have some combination of low inclination, small mass ratio, large eccentricity, and larger radial velocity uncertainties. If, for the sake of argument, we ignore the excess of short-period systems and assume that the $\beta \sim 0$ power-law holds, the ~ 15 binaries in the 1–10 day period range would imply an equivalent number between 10 and 100 days. There are 8 known systems in this range, leaving an additional 7 putative binaries as undetected. The mean completeness over this range is $\sim 82\%$, suggesting that ~ 12 of the 15 would be detectable by our survey. This implies that the ongoing Cyg OB2 survey should uncover as many as ~ 5 additional binaries with periods between 10 and 100 days, given sufficient long-term data. For periods longer than 100 days, where there are presently only two systems with orbital solutions, Schulte 9 (Nazé et al. 2010) and MT070 (Paper VI), detection becomes more difficult. In the case of Schulte 9, with a period of ~ 2.355 years and an eccentricity of nearly 0.7, even an observing campaign such as this one experienced difficulty in uncovering this massive “twin” system. All of the foregoing discussion, however, assumes an Öpik period distribution, and we have already shown in Figure 4 that no single power-law adequately reproduces the data at the shortest periods, $P < 14$ days.

4.2. Eccentricity Distribution

Observationally, binaries with solar-type primaries and periods longer than a year have a broad distribution of orbital eccentricities with a median value of 0.55 (Duquennoy & Mayor 1991). For periods shorter than this, these systems have a higher concentration near zero eccentricity stemming from circularization of the orbits. This is also shown to be true for O-star binaries with periods as long as 10,000 days (Sana & Evans 2011). Although the method by which binary orbits are circularized and the critical period below which all are circular is unclear from existing data, a standard eccentricity versus period scatter diagram, like Figure 2, illustrates that binaries with short periods do tend toward nearly circular orbits. The figure shows a decline of mean eccentricity for periods under 10 days. Giuricin et al. (1984) found that nearly all (92%) early-type binaries with periods shorter than two days had an eccentricity less than 0.05. They also found that the eccentricities of nearly all of the early-type binaries in their survey could be explained by the Zahn (1977) tidal theory, which describes the circularization time for an equal mass binary with an initial eccentricity of $e < 0.3$ as being related to the main sequence lifetime of that binary. Khaliullin & Khaliullina (2010) provide a modified version of the Zahn (1977) theory and

address the evolution of the orbital parameters over the circularization time of the orbit. The circularization timescales are, on average, a third of those predicted by Zahn (1977) and in better agreement than the predictions of Tassoul (1988) with the massive star binary statistics of Giuricin et al. (1984). The predicted circularization time for an early-type (pair of B0V stars), nearly equal-mass binary at a separation comparable to the Cyg OB2 early B-type binaries (e.g., *asini* ~ 0.16 AU for MT720) is close to the main-sequence lifetime of an early B star. However, a study by Witte & Savonije (2001) found that there are a significant number of early-type binaries with periods up to 10 days with an eccentricity near zero that cannot be explained with the Zahn (1977) theory and are unlikely to have been primordially circular. Krumholz & Thompson (2007) have proposed a method by which orbits become significantly circularized during the star formation process, thereby diminishing the conflict between circularization time and the theoretical life span of massive stars. However, the theory assumes the binary is formed concurrently with the formation of the components, and that is a highly debated topic in massive star formation theory (Zinnecker & Yorke 2007).

In Figure 6 we show the MC code best fit to the Cyg OB2 eccentricity distribution. As in Figure 4, diamonds show the normalized cumulative distribution (left Y-axis) and the solid curve shows the normalized cumulative distribution for $\gamma = -0.6$. Figure 3 (upper left and right panels) shows that the index γ is confined, at the 1σ level, to $-1.0 < \gamma < -0.4$ with a best fit of $\gamma = -0.6 \pm 0.3$. The steep negative power-law is required to reproduce the abundance of systems with low eccentricity. A K-S test shows that the $\gamma = -0.6$ power law is compatible (i.e., the observed sample and the synthetic sample are consistent with being drawn from the same parent distribution) with the data at the $\sim 90\%$ level. The absence of eccentricities with $e > 0.55$ is similar to what is observed for short-period binaries in other OB clusters (e.g. NGC 6231; Sana et al. 2008). Highly eccentric systems are apparently rare in this period regime, either because circularization mechanisms are efficient, or possibly because they are more easily disrupted during encounters with other cluster stars. Finally, we note that the eccentricity distribution within Cyg OB2 is also compatible with that of OB binaries in the 9th Spectroscopic Binary Catalog at the $\sim 50\%$ level.

We show an estimate of the survey completeness as a function of eccentricity for two different period ranges in Figure 7. The solid and dot-dash curves represent the completeness for $P < 1000$ days and $P < 30$ days respectively. The plot indicates that the survey is $\sim 75\%$ complete at $e \sim 0.65$ for binaries with $P < 1000$ days and $\sim 88\%$ complete at $e \sim 0.75$ for binaries with $P < 30$ days. For $P < 30$ days, the survey is likely to have detected the vast majority of systems, even those with large eccentricities, if they exist.

4.3. Mass Ratio Distribution

The nature of the mass ratio distribution is one of the more highly debated and unresolved questions pertaining to massive binaries and their formation. The distribution is difficult to characterize because of the unavoidable bias of observational studies, including this one, against low- q systems. The general consensus is that short-period binaries have a different mass ratio distribution compared to the long-period binaries. Goldberg et al. (1991) and Duquennoy & Mayor (1991) show this with lower-mass binaries, but they also point out that the period range over which this change occurs is still ill-defined. Most studies on the mass ratio distribution are for mid to late-type stars. A few examples include Duquennoy & Mayor (1991), who find $\alpha \leq -2$ (for $q > 0.1$ and periods 1–10,000+ days) for a large survey of solar-type spectroscopic binaries, Kouwenhoven et al. (2007), who find $\alpha = -0.4$ to -0.5 for a large survey of spectroscopic and visual A- and B-type primaries in Sco OB2, Fisher et al. (2005), who find $\alpha \sim 0$ for all the SB1s and $\alpha > 0$ for all the SB2s in the solar neighborhood (for periods 1–500 days), and Hogeveen (1992), who find $\alpha \simeq 0$ for mass ratios of $q < 0.3$ and $\alpha \leq -2$ for mass ratios of $q \gtrsim 0.3$ in binaries of B-type and later (for periods <1 day to 10,000+ days). Among the massive stars, studies such as Pinsonneault & Stanek (2006) conclude from their study of 21 eclipsing massive binaries ($P < 5$ days) in the Small Magellanic Cloud, that the secondary mass function for massive binaries does not follow a Salpeter (1955) slope. Instead, the authors find a flat distribution of mass ratios and predict that roughly 55% of all massive systems are part of a “twin” system with a mass ratio of $q > 0.95$. Sana & Evans (2011) have refuted this proposition, but also find a preference for more massive companions among O-stars in clusters.

The distribution of observed mass ratios in Cyg OB2, shown in Figure 1, appears relatively flat, except for a slight preference for mass ratios between 0.7 and 0.9. This may be an artifact of using a standard histogram for small numbers. Not surprisingly, the upper end of the distribution is populated exclusively by SB2s, while the lower end of the distribution is almost entirely populated by SB1s. For five of these single-lined systems, we calculated the expected orbital inclination, $\langle i \rangle$, between i_{MIN} and 90° , using the inclination lower limits estimated from Paper II, Paper III, and Paper VI. We calculate the most probable mass ratios to be 0.27, 0.30, 0.03, 0.22, and 0.11 for MT059, MT145, MT174, MT258, and MT267, respectively. These are close to the lower-limit values for q because $\langle i \rangle$ is not far from the upper limit on i . There is a possibility, of course, that for one or more of these systems, the orbital inclination could be less than $\langle i \rangle$, and therefore, the system(s) would have a more massive companion. In such a case, our present estimates may incorrectly inflate the number of systems with mass ratios between 0.05 and 0.30, and the true distribution would not be as flat as currently shown in Figure 1.

From the MC code we find a best fit of $\alpha = 0.1 \pm 0.5$ for the mass ratio distribution. Figure 8 shows the normalized cumulative distribution of mass ratios (diamonds), along with the corresponding simulated cumulative distribution for $\alpha = 0.1$ (thick curve). The 1σ contours (top left and bottom left panels in Figure 3) show a range of $-0.3 < \alpha < 0.7$. Such a shallow positive power-law indicates that mass ratios in the cluster are quasi-uniformly distributed between $q = 0.005$ and $q = 1.0$ with a preference for larger mass ratios. This type of distribution implies that the secondaries are not drawn from a Salpeter (1955) stellar IMF, in contrast to lower-mass binary populations which exhibit an abundance of low mass ratios. Furthermore, the histogram of mass ratios in Figure 8 is also inconsistent with the “twin-heavy” population suggested by Pinsonneault & Stanek (2006), whereby 45% of systems are predicated to have $q > 0.95$.

Figure 9 shows the completeness of the survey as a function of mass ratio. For systems with $P < 30$ days (dot-dash curve), the survey is at least 90% complete down to $q \sim 0.25$, but there is a sharp drop in the fraction of systems detected for $q \lesssim 0.25$. The average completeness is 10–20% lower, overall, for longer period systems with $P < 1000$ days (solid curve). Our measurement of MT174 ($q = 0.03$; $K_1 = 9 \text{ km s}^{-1}$) below our nominal semi-amplitude detection threshold of 15 km s^{-1} provides evidence that such low-amplitude, low- q systems exist and are detectable in our survey. Figure 9 shows that incompleteness is an issue only at the lowest mass ratios. Any attempt to correct for incompleteness at $q < 0.25$ would add low- q systems to the histogram and serve to flatten the distribution.

4.4. Binary Fraction

Table 2 shows a selection of the larger surveys that investigated the O-star binary fraction within individual clusters/associations. Column 1 contains the common cluster identification, column 2 is the number of O stars included in the survey, column 3 is the number of early B stars included in the survey, column 4 is the lower limit on the O-star binary fraction, column 5 is the lower limit on the massive star binary fraction (O and early-B primaries), and column 6 references the original works. The observed O-star binary fractions (designated *b.f.* rather than *B.F.* here to distinguish from the intrinsic binary fraction) within the clusters listed range widely from 0 – 67% (column 4). More inclusively, the massive star *b.f.* (with primaries B3 and earlier; column 5), varies between 4% (NGC 330 in the SMC) and 53% (NGC 6231). In Paper I, we find an initial lower limit on the binary fraction of 30% based on the χ^2 probability density function for radial velocities from the first six years of observations of Cyg OB2, which would place it near the middle of the binary fraction range among massive stars. KF07 find a more probable binary fraction of *B.F.* $> 70\%$ based on

their Monte Carlo analysis of the raw radial velocities, which would place it closer to that of NGC 6231. However, based purely on the binary detections of Papers II–IV & VI, the hard lower limit on the binary fraction among massive stars in Cyg OB2 is 21% (i.e., 24/114).

We show the observed χ^2 probability density function (PDF) for the radial velocities of Cyg OB2 stars in Figure 10. There are 53 having $P(\chi^2, \nu) < 5\%$ and 43 with $P(\chi^2, \nu) < 1\%$. These systems encompass the 24 known binary systems and additional candidates for radial velocity variables. The number of variables has increased from Paper I despite removing some low S/N spectra that may have caused extraneous velocities. This is understandable given the additional data acquired on the sample, especially on long period binaries like MT070 ($P = 7.58$ years). Figure 11 shows the MC code best fit to the cumulative χ^2 PDF for radial velocities in Cyg OB2 using the “unbiased” sample of 110 stars. The solid curve represents the cumulative χ^2 PDF produced by the MC code with best-fit indices of $\alpha = 0.1$ ($q_{MIN}=0.005$), $\beta = 0.4$ ($P_{MAX}=1000$ days), and $\gamma = -0.6$ ($e_{MIN}=0.0001$, $e_{MAX}=0.9$). The open diamonds represent the normalized cumulative χ^2 PDF for the unbiased sample of OB primaries. The best MC code fit results in a binary fraction of $B.F. = 45 \pm 8\%$ if all binary systems are assumed to have $P < 1000$ days. Simulated binary populations with binary fractions of 40–50% in increments of 1% and with fixed α , β , and γ , were individually examined for better agreement with the data. These additional simulations show that a binary fraction of 44% yields a slightly better fit to the data.

Figure 12 shows the results of the Monte Carlo analysis for the 18 OB close binaries comprising the “unbiased” sample. Similar to Figure 3, the four panels provide the 1σ , 2σ , and 3σ probability contours for α , β , γ , and binary fraction. The three panels depicting probabilities for power-law indices (upper left, upper right, lower left) are nearly identical to the results from the MC analysis of the “complete” sample shown in Figure 3. The best-fit β is slightly larger (0.4 instead of 0.2) owing to the exclusion of several shorter-period binaries from the unbiased sample. The best-fit α and γ are the same, just with larger uncertainties. The contours in the lower right panel show that the binary fraction is confined to $37\% < B.F. < 49\%$ at the 1σ level and $30\% < B.F. < 60\%$ at the 3σ level for $P_{MAX} = 1000$ days. This result is consistent with the range of massive binary fractions for Galactic clusters listed in Table 2. In order to compare our current results to the Monte Carlo analysis of KF07, who explored a larger range of periods (separations of 0.02–10,000 A.U. corresponding to $P \sim 1-10^7$ days for two $20 M_{\odot}$ stars), we also performed a MC run with $P_{MAX} = 10^7$ days. In both analyses 10,000 A.U. is considered a reasonable upper limit for bound systems. In this case, we find the binary fraction must be $\sim 100\%$ in order to replicate our observed χ^2 PDF. This is in rough agreement with the conclusions of KF07, but based on extrapolating the power-law distributions of mass ratios and periods determined from close binaries over many orders of magnitude to characterize loosely bound systems.

Is an extrapolation of the power law index β to periods as long as 10^7 days warranted when our radial velocity survey is sensitive only to systems with periods less than about 10 years? Caballero-Nieves et al. (2011) conducted an adaptive optics and *HST* Fine Guidance Sensor survey of 75 Cyg OB2 systems and detect highly probable companions around 31 OB primaries at separations >200 A.U. ($P > 630$ years). Of these, nine ($9/75 = 12\%$) have probable periods in the range 10^3 – 10^4 years (S. Caballero-Nieves, private communication)². If we adopt $P_{MAX} = 10^4$ years ($\sim 365,250$ days), the MC code provides a best fit binary fraction of $\sim 90\%$, and this extrapolation of the $\beta \simeq 0.2$ power law predicts approximately 15 binaries with orbital periods in each 1 dex interval (i.e., 15 with periods between 10 yr and 100 yr, 15 between 100 yr and 1000 yr, etc.) given the 110 stars in our unbiased sample. This translates into about 14% of the binary systems falling within each logarithmic period interval. Hence, the predictions of an extrapolated power-law appear consistent with the emerging high angular resolution observations at larger separations. We therefore suggest that the binary fraction among massive stars may be as high as $90 \pm 10\%$ if periods as long as 10^4 years are allowed.

4.5. Sensitivity to other model assumptions

In addition to exploring the effect of varying P_{MAX} , we also examined the effect of varying q_{MIN} and the semi-amplitude detection threshold, K_{MIN} , in the MC code. As K_{MIN} is changed from 15 km s^{-1} to 20 km s^{-1} or larger, a greater fraction of synthetic systems are deemed undetectable by the code, and the detected systems have smaller separations and/or larger companions. Therefore, we expect some combination of increase in α (larger mass ratios), decrease in β (shorter periods), and increase in binary fraction. We find insignificant change (i.e., α , β , γ are the same) when $K_{MIN} = 20 \text{ km s}^{-1}$. A significant change in the indices is not observed until K_{MIN} is increased to much larger values of $\sim 50 \text{ km s}^{-1}$. We are also confident our detection threshold is much closer to 15 km s^{-1} , as evidenced by the measurement of MT070 (Kobulnicky et al. 2012). We conclude that the minimum semi-amplitude for binary detection is appropriately set at 15 km s^{-1} .

In the case of increasing q_{MIN} , the lowest mass ratio simulated in the code, we primarily expect to see a decrease in α and a decrease in the binary fraction. Binaries will have more massive companions and semi-amplitudes will be larger, meaning that a smaller fraction of binary systems will be deemed undetectable in the code. We observed only a small decrease

²We use a distance of 1700 pc, correct statistically for projection effects, and assume a total system mass of $30 M_{\odot}$ to turn the angular separations into estimated periods.

in binary fraction in runs with $q_{MIN} = 0.1$ (a few percent and still consistent with our initial results). We also find only a small increase in α and no change in β or γ . However, increases in α become larger when $q_{MIN} > 0.1$. For example, α changes from 0.1 to -0.4 for the “complete” sample when $q_{MIN} = 0.2$; however, such a large q_{MIN} is probably unphysical given the existence of MT070 ($q \geq 0.03$) and MT267 ($q \geq 0.11$). These results, for both tests, indicate that our MC results are not sensitive to small changes in the adopted values of the mass ratio lower limit or semi-amplitude threshold.

5. Discussion

5.1. Possible Origin of the Short-Period Excess

The presence of an excess of binary systems with periods around 3–5 days (with a peak at 4–5 days) and a shortage of systems with periods around 7–14 days is not only observed in Cyg OB2. Sana et al. (2008) observe a similar occurrence in NGC 6231, and the excess and shortage of systems occur at roughly the same ranges in period. Systems in Cyg OB2 that lie within the excess encompass a range of spectral types, mass ratios, and binary types (i.e., eclipsing, SB1 and SB2) and are scattered randomly across the cluster, having no preferred location either in dense or sparse regions. We do not believe this peculiar distribution can be attributed to observational biases given the extended time coverage of this survey and the different observing cadences of the observing runs that have contributed to the Cyg OB2 binary catalog. While the existence of an excess of systems with periods of around 3–5 days seems well-established in the literature and in our present data, the possibility of a shortage in the 7–14 day range has not been previously noted. A comparison between the Cyg OB2 cumulative period distribution with the data from Garmany et al. (1980) reveals a flattening in this 7–14 day range (though we should be cautious given the use of a standard histogram and small numbers). Their survey (of 28 systems) contains three in this 7–14 day range while ours (22 systems) contains one.

While we find that no single power-law can adequately describe the log-period distribution in Cyg OB2, it is unlikely, given any power-law distribution, to find so few systems between 7 and 14 days. We examined the probability that only a single system would be observed in the 7–14 day period range given a random drawing of 22 systems with $1.46 < P < 25.2$ days (for $\beta = -1$ to 1). Random samples were drawn 10,000 times and the final percentages were adjusted for a 90% completeness level (the mean level as measured in Figure 5 for the 7–14 day range). The likelihood of detecting a single system for $\beta = 0$ is $\sim 2\%$. However, if the power-law describing the log-period distribution is assumed to be closer to -1 , then the probability rises quickly to $\sim 13\%$ (with $\sim 5\%$ for $\beta = -0.5$, and

$< 1\%$ for $\beta = 0.5$ and 1). This tells us that if the power-law(s) that describe the log-period distribution have $\beta \geq -0.5$, the shortage is a real phenomenon at the 2σ level.

In an attempt to replicate the Cyg OB2 period distribution with a physically motivated prescription, we made a version of the Monte Carlo code to take 70% of the systems assigned a period between 7 and 14 days and reassign them assuming the same power-law describing the rest of the distribution to periods between 3 and 5 days. The 70% reassignment fraction reflects a 90% completeness level and detection of one out of a probable 3 or 4 systems in this range. This approach approximates what would happen if binary systems with periods 7 and 14 days migrated to shorter periods. The best fit using this approach is shown in Figure 13 and comes from reassigning systems with a period between 7 and 13.5 days to a period between 4 and 5 days (corresponding to the peak of the excess in the Cyg OB2 distribution) with only a slight increase in β (0.5 and within the uncertainty of our results). α , γ , and the binary fraction are same as in Section 4. The normalized cumulative distribution for the Cyg OB2 data is represented by the diamonds and the solid curve represents the normalized cumulative period distribution for the best fit using this version of the MC code. Though this fit requires a slightly more positive slope for the initial period distribution, the overall fit to the data is visually better than in Figure 4, and the multiple changes in the slope are also replicated well. A two-sided K–S test yields a compatibility of greater than 99% (compared to $\sim 60\%$ with the simple power-law approach).

A plausible explanation for such period migration could be the mechanism proposed by Krumholz & Thompson (2007) whereby the circularization of the orbit occurs primarily during the formation process instead. In Figure 14 we show the evolution of orbital period/semi-major axis and mass ratio for a binary system with a total mass of $30 M_{\odot}$ as the primary loses mass to the secondary. The plotted curves show tracks of constant angular momentum as systems evolve toward shorter periods with mass ratios approaching unity, assuming that mass and angular momentum are conserved,

$$\frac{a}{a_0} = \left(\frac{q_0}{q}\right)^2 \left(\frac{1+q}{1+q_0}\right)^4, \quad (1)$$

(e.g., equation 8 of Krumholz & Thompson 2007). Here a_0 and q_0 are the initial semi-major axis and mass ratio while a and q are the final semi-major axis and mass ratio after mass transfer. The two solid curves are tracks for systems with initial mass ratios $q = 0.5$ and initial periods of 7 and 14 days. These systems may end up having mass ratios near unity, but their final periods are longer than 5 days. The dotted curves are tracks for systems that begin with mass ratios $q = 0.3$ and periods of 7 and 14 days. These systems may end up with mass ratios near unity and periods in the range 3–5 days. This is precisely

where we observe an excess of systems with short periods in Cyg OB2, and we also find a relative abundance of systems with mass ratios $q = 0.8\text{--}0.9$ — not exactly “twins”, but systems where significant mass transfer may have taken place. This figure indicates that, if the Krumholz & Thompson (2007) mechanism is the operative one producing an abundance of short-period, high- q systems, then some fraction of the population of 3–5 day systems should originate as systems with $q \simeq 0.3$ with 7–14 day periods. While the evidence for “missing” 7–14 day systems in Cyg OB2 is compelling, we cannot claim, on the basis of the present data, to see the corresponding lack of systems with $q \simeq 0.3$. Our survey is sufficiently incomplete in this mass ratio range that observational biases preclude any firm conclusion.

5.2. Role of Close Binaries in Energetic Phenomena

The Cyg OB2 radial velocity survey originated as an observational effort to inform theoretical models predicting the frequency of energetic events like supernova and γ -ray bursts that may have close binaries as progenitors. A key ingredient of these modeling efforts is the fraction of massive stars that might interact through mass transfer or undergo a common envelope phase, especially during the post-main-sequence evolution of either star in the system. Red supergiants are the descendants of massive stars, so we adopt the RSG radii deduced by Levesque et al. (2005) which range between $200 R_{\odot}$ and $1500 R_{\odot}$. Their Figure 3 shows stellar evolutionary tracks indicating that stars in the mass range $15 - 30 M_{\odot}$ may reach or exceed $1000 R_{\odot}$ while stars with initial masses over $10 M_{\odot}$ can generally be expected to reach $500 R_{\odot}$. We adopt $500 R_{\odot}$ as a maximum evolved radius for stars in our sample, meaning that systems with semi-major axes smaller than this value will interact strongly, probably through the formation of a common envelope. Other systems may interact via mass transfer after Roche Lobe overflow. Eggleton (1983) provides an analytic description of the Roche Lobe radius as a function of mass ratio. His tabulated values show that the Roche Lobe radii for binary systems with mass ratios $q = 0.2 - 1.0$ fall in the range $0.38a - 0.55a$ where a is the separation of the components. Consequently, we adopt $1000 R_{\odot}$ (4.7 A.U.) as a conservative threshold separation, below which systems are deemed to interact during the evolution of the system. In our Monte Carlo code, we flag all systems with periastron distances less than $1000 R_{\odot}$ as capable of interaction. Assuming $\alpha = 0.1$, $\beta = 0.2$, $\gamma = -0.6$, and $P_{MAX} = 10^4$ years, this predicts that 45% of the binary systems will have sufficiently close companions to interact during the binary’s lifetime (37% if we adopt the slightly larger $\beta = 0.5$ from Section 5.1).

5.3. The Luminosity Contribution from Secondaries

The luminous contribution from secondary stars, which are unresolved in photometric surveys, even with the *HubbleSpaceTelescope* or adaptive optics, is not negligible. Consequently, measuring accurate distances to star clusters using spectroscopic parallax, main sequence fitting, or similar standard-candle techniques is systematically in error if close companions are neglected. As part of our Monte Carlo code we tallied the mean V-band light contribution from primary and secondary stars by using a zero-age main sequence (ZAMS) relation between stellar mass and absolute V magnitude (Martins et al. 2005; Drilling & Landolt 2000). For the best fitting power law indices described above, allowing for periods as long as 10^4 yr, we find that the secondary stars contribute 16% of the total stellar light at V-band. This is equivalent to a systematic error in the distance modulus of 0.16 mag and a systematic distance error of about 8%, in the sense that distances derived without correcting for luminous secondaries will be too small. We expect the secondary luminosity fractions in evolved populations to vary stochastically about this 16% ZAMS value as the primary and secondary components throughout the population become giants and supergiants. The intricacies of mass exchange between components will further limit any simple description of the time evolution in the nominal ZAMS value.

6. Conclusions

In this, our fifth work of this series, we present the results of a Monte Carlo analysis using a decade of radial velocity data on 114 massive stars in the Cyg OB2 Association. This survey is unique in terms of number of massive stars and binary solutions analyzed. It improves on KF07 and other works (e.g., Evans et al. 2006, Garmany et al. 1980, Gies 1987, Pourbaix et al. 2004) in that we utilize the radial velocity information obtained over a larger time span and make use of the nearly complete orbital information—including eccentricities—on 22 of the 24 known massive binaries. The Cyg OB2 binaries have been observed by spectroscopic and/or photometric means and cover a period range of 1.47 days – 7.58 years (with all but a few having $P < 26$ days), an eccentricity range of 0–0.53, and a mass ratio range of 0.03–0.99. On the strength of these data, we compute the binary fraction for a large, young population (2–3 Myr) of massive stars from a common origin. In addition, we use this information to model the most probable intrinsic distributions for period, mass ratio, and eccentricity for short-period systems having $P < 26$ days.

- The data imply a hard lower limit on the binary fraction of 21% (i.e., 24/114 systems). The Monte Carlo analysis of the unbiased sample of 110 OB stars (i.e., not including

A36, A45, B17, and Schulte 5), indicates a massive star binary fraction of $44 \pm 8\%$, assuming that the allowed period range is 1–1000 days (separations $\sim 0.01 - \text{few} \times 10$ AU). However, if we extrapolate the best fit power-law distributions over several orders of magnitude and allow for periods as long as 10^4 years, the binary fraction may be as large as $90 \pm 10\%$. These results are consistent with the probable number of binaries detected in the adaptive optics and *HST* survey of Cyg OB2 by Caballero-Nieves et al. (2011) and with the previous results of KF07.

- The best-fitting distributions of mass ratio, period, and eccentricity are described by power-laws with indices $\alpha = 0.1 \pm 0.5$, $\beta = 0.2 \pm 0.4$, and $\gamma = -0.6 \pm 0.3$, respectively, assuming lower and upper bounds on the power-law distributions of $q=0.005-1.0$, $P=1-1000$ days, and $e=0.0001-0.9$. These values for α and β are broadly consistent with the previous results of KF07, as well as Sana et al. (2008), Kouwenhoven et al. (2007), Garmany et al. (1980), and the analysis of Sana & Evans (2011). The mass ratio distribution is not consistent with the “twin-heavy” population proposed by Pinsonneault & Stanek (2006), but suggests a weak preference for larger mass ratios (i.e., $q \geq 0.8$).
- The distribution of orbital periods is not consistent with any single power-law, owing to a significant excess of systems with periods around 3–5 days (peaking at 4–5 days) and a deficit of systems with periods around 7–14 days. Such a 3–5 day excess has been observed among massive stars in NGC 6231 (Sana et al. 2008), but the latter phenomenon has not been previously reported. We propose that it may stem from binary systems with periods initially in the range of $\sim 7-14$ days migrating to shorter periods during a period of pre-main-sequence mass transfer, via the mechanism proposed by Krumholz & Thompson (2007).
- The fraction of massive-star binaries (or higher order systems) having companions close enough to interact during pre- or post-main-sequence evolution, defined here as requiring a semi-major axis < 4.7 AU ($\sim 1000 R_{\odot}$), is $\sim 45\%$. This fraction is a key ingredient in recipes that predict the cosmic rates of binary-induced phenomena arising from massive stars, such as some classes of supernova and γ -ray bursts.

We present these findings in the anticipation that they, along with the analyses of other clusters (such as the work with Sco OB2 by Kouwenhoven et al. 2007, NGC 6231 by Sana et al. 2008, NGC 2244 by Mahy et al. 2009, and NGC 6611 by Sana et al. 2009), will aid our understanding of numerous issues involving massive stars, including their formation, the predicted rates of supernovae type Ib/c arising through binary channels, and whether there is a correlation between cluster density and the binary fraction therein. This ongoing survey

will continue to uncover massive spectroscopic binaries in Cyg OB2. These new SB1s and SB2s will help refine our characterization of the orbital parameter distributions and increase our understanding of the nature of the excess in orbital periods between ~ 3 –5 days. While the present data has provided solid constraints on the massive binary characteristics in Cyg OB2, it is possible that the binary fraction or distribution of periods/mass ratios/eccentricities varies temporally as a cluster ages or is a function of initial cluster density. Discerning whether these additional variables are important will require more extensive surveys over a range of age and formation environment.

We would like to acknowledge the helpful advice and attention to detail we received from our referee in the process of making this a much better manuscript. We thank Mark Krumholz and Hans Zinnecker for inspiring conversations about phenomena in short-period binaries, Chris Fryer for helpful discussions regarding interacting binary systems, and Saida Caballero-Nieves for sharing her imaging data of Cyg OB2 in advance of publication. We are very appreciative for the continued advice and encouragement throughout the project from Ginny McSwain. Additionally, we are grateful for the continued support from the National Science Foundation through Research Experience for Undergraduates (REU) program grant AST 03-53760, through grant AST 03-07778, AST 09-08239, and the support of the Wyoming NASA Space Grant Consortium through grant NNG05G165H.

Facilities: WIRO (), WIYN (), Shane (), Keck:I ()

REFERENCES

- Blaauw, A. 1961, BAN, 15, 265
- Caballero-Nieves, S. M., Gies, D. R., Roberts, L. C., & Turner, N. H. 2011, Bulletin Société des Sciences de Liège, 80, 639
- Clark, J. S., Ritchie, B. W., & Negueruela, I. 2010, A&A, 514, 87
- Comerón, F., Pasquali, A., Figueras, F., Torra, J. 2008, A&A, 486, 453
- Comerón, F., et al. 2002, A&A, 389, 874
- De Becker, M., Rauw, G., Manfroid, J., & Eenens, P. 2006, A&A, 456, 1121
- Drew, J. E., Greimel, R., Irwin, M. J., Sale, S. E. 2008, MNRAS, 386, 1761
- Drilling, J. S., & Landolt, A. U. 2000, in Astrophysical Quantities, ed. A. N. Cox (4th ed.; New York; Springer), 381

- Duquennoy, A., & Mayor, M. 1991, *A&A*, 248, 485
- Duchêne, G., Simon, T., Eislöffel, J., & Bouvier, J. 2001, *A&A*, 379, 147
- Eggleton, P. P. 1983, *ApJ*, 268, 368
- Evans, C. J., Lennon, D. J., Smartt, S. J., & Trundle C. 2006, *A&A*, 456, 623
- Fisher, J., Schröder, K. P., & Smoth, R. C. 2005, *MNRAS*, 361, 495
- Fryer, C. L., Woosley, S. E., & Hartmann, D. H. 1999, *ApJ*, 526, 152
- Garcia, B., & Mermilliod, J. C., 2001, *A&A*, 368, 122
- Garmany, C. D., Conti, P. S., & Massey, P. 1980, *ApJ*, 242, 1063
- Gies, D. R., 1987, *ApJS*, 64, 545
- Giuricin, G., Mardirossian, R., & Mezzetti, M. 1984, *A&A*, 134, 365
- Goldberg, D., Mazeh, T., & Latham, D. W. 1991, *ApJ*, 591, 397
- Hillwig, Todd C., Gies, Douglas R., Bagnuolo, William G., Jr., Huang, Wenjin, McSwain, M. Virginia, Wingert, David W. 2006, *ApJ*, 639, 1069
- Hogeveen, S. J. 1992, *Ap&SS*, 196, 299
- Khaliullin, Kh. F., & Khaliullina, A. I. 2010, *MNRAS*, 401, 257
- Kiminki, D. C., Kobulnicky, H. A., Kinemuchi, K., Irwin, J. S., Fryer, C. L., Berrington, R. C., Uzpen, B., Monson, A. J., Pierce, M. J., & Woosely, S. E. 2007, *ApJ*, 664, 1102
- Kiminki, D. C., Kobulnicky, H. A., Gilbert, I., Bird, S., & Chunev, G. 2009, *AJ*, 137, 4608
- Kiminki, D. C., Kobulnicky, H. A., Ewing, I., Lundquist, M., Alexander, M., Vargas-Alvarez, C., & Choi, H. 2010, *ApJ*, 745, 1
- Kiminki, D. C., McSwain, M. V., & Kobulnicky, H. A. 2008, *ApJ*, 679, 1478
- Kobulnicky, H. A., & Fryer, C. L. 2007, *ApJ*, 670, 747
- Kobulnicky, H. A., Smullen, R., Kiminki, D. C., Long, G., & Runnoe, J. 2012, in prep
- Kouwenhoven, M. B. N., Brown, A. G. A., Portegies Zwart, S. F., & Kaper, L. 2007, *A&A*, 474, 77

- Krumholz, M. R., & Thompson, T. A. 2007, *ApJ*, 661, 1034
- Kurtz, M. J., Mink, D. J., Wyatt, W. F., Fabricant, D. G., Torres, G., Kriss, G. A., & Tonry, J. L. 1991, in *Astronomical Data Analysis Software and Systems I*, ASP Conf. Ser., Vol. 25, eds. D.M. Worrall, C. Biemesderfer, and J. Barnes, p. 432
- Law, D. R., Steidel, C. C., Erb, D. K., Larkin, J. E., Pettini, M., Shapley, A. E., & Wright, S. A. 2009, *ApJ*, 697, 2057
- Lejeune, T., & Schaerer, D. 2001, *A&A*, 366, 538
- Levesque, E. M., Massey, P., Olsen, K. A. G., et al. 2005, *ApJ*, 628, 973
- Linder, N., Rauw, G., Manfroid, J., Damerdji, Y., De Becker, M., Eenens, P., Royer, P., & Vreux, J. M. 2009, *A&A*, 495, 231
- Mahy, L., Nazé, Y., Rauw, G., Gosset, E., M. De Becker, Sana, H., & Eenens, P. 2009, *A&A*, 502, 937
- Maíz-Apellániz, J., Walborn, N. R., Galué, H. Á., & Wei, L. H. 2004, *ApJS*, 151, 103
- Maíz Apellániz, J. 2010, *A&A*, 518, A1
- Martins, F., Schaerer, D., & Hillier, D. J. 2005, *A&A*, 436, 1049
- Mason, B., Hartkopf, W. I., Gies, D. R., Henry, T. J., & Helsel, J. W. 2009, *ApJ*, 137, 3358
- Massey, P., & Thompson, A. B. 1991, *AJ*, 101, 1408
- Mermilliod, J. C. 1995, in *Information & On-Line Data in Astronomy*, ed. D. Egret, & M. A. Albrecht (Kluwer Academic Publishers, Dordrecht), 127
- Miller, G. E., & Scalo, J. M. 1979, *ApJS*, 41, 513
- Nazé et al. 2010, *ApJ*, 719, 634
- Öpik, E. J. 1924, *Tartu Obs. Publ.*, 25
- Pigulski, A., & Kolaczowski, Z. 1998, *MNRAS*, 298, 753
- Pinsonneault, M. H., & Stanek, K. Z. 2006, *ApJ*, 639, 67
- Podsiadlowski, Ph., Joss, P. C., & Hsu, J. J. L. 1992, *ApJ*, 391, 246
- Pourbaix, D., et al. 2004, *A&A*, 424, 727

- Rauw, G., & De Becker, M. 2004, *A&A*, 421, 693
- Salpeter, E. E. 1955, *ApJ*, 121, 161
- Sana, H., & Evans, C. J. 2011, *IAUS*, 272, 474
- Sana, H., Gosset, E., & Evans, C. J. 2009, *MNRAS*, 400, 1479
- Sana, H., Gosset, E., Nazé Y., Rauw, G., & Linder, N. 2008, *MNRAS*, 386, 447
- Sana, H., Momany, Y., Gieles, M., et al. 2010, *A&A*, 515, A26
- Schulte, D. H. 1958, *AJ*, 128, 41
- Stroud, V. E., Clark, J.S., Negueruela, I. , Roche, P., & Norton, A.J. 2009, *A&A*, 511, 84
- Tassoul, J. 1988, *ApJ*, 324, 71
- Turner, N. H., ten Brummelaar, T. A., Roberts, L. C., et al. 2008, *AJ*, 136, 554
- Witte, M. G., & Savonije, G. J. 2001, *A&A*, 366, 840
- Wright, N. J., Drake, J. J., Drew, J. E., & Vink, J. S. 2010, *ApJ*, 713, 871
- Zahn, J. P. 1977, *A&A*, 57, 383
- Zinnecker, H., & Yorke, H. W. 2007, *ARA&A*, 45, 481

Table 1. Ephemerides for Cyg OB2 Stars Used in Monte Carlo Analysis

Star	Date HJD-2,400,000	V_r (km s ⁻¹)	σ_V (km s ⁻¹)
A36	54,403.61	-163.4	5.6
A36	54,403.70	-174.9	5.0
A36	54,405.71	103.4	5.3
A36	54,406.63	105.4	3.7
A36	54,406.76	108.6	3.7

Note. — Column 1 gives the star designation in either Schulte (1958) (S), Comerón et al. (2002) (A,B) or Massey & Thompson (1991) (MT) format. Column 2 gives the heliocentric Julian date in the format HJD-2,400,000. Column 3 gives the cross-correlation velocity in km s⁻¹. Column 4 gives the 1 σ cross-correlation error in km s⁻¹. Table 1 is published in its entirety in the electronic edition of the *Astrophysical Journal*. A portion is shown here for guidance regarding its form and content.

Table 2. Massive Star Binary Statistics

Cluster ID	O Stars in Survey	Early-B Stars in Survey	<i>b.f.</i> (O-Stars)	<i>b.f.</i> (Massive Stars)	Reference ID
NGC 2004 (LMC)	4 (1)	83 (21)	25%	25%	1
NGC 330 (SMC)	6 (0)	76 (3)	0%	4%	1
NGC 346 (SMC)	19 (4)	59 (19)	21%	29%	1
Trumpler 14	7 (1)	...	14%	...	2,3
IC 1805	10 (2)	...	20%	...	4,5
NGC 2244	6 (1–2)	...	17–33%	...	6
NCC 6231	16 (10)	33 (16)	63%	53%	2,7
NGC 6611	9 (4)	...	44–67% ^a	...	2,3,8
IC 2944	16 (7)	...	44%	...	2,3
Trumpler 16	20 (7)	...	35%	...	2,3
Cr 228	21 (5)	...	24%	...	2,3
Cyg OB2	44 (12)	69 (8)	27%	18%	9,10,11

Note. — A selection of OB cluster/association studies examining the binary fraction of massive stars. The number of binaries are shown in parentheses.

References. — (1) Evans et al. (2006); (2) Garcia & Mermilliod (2001); (3) Mermilliod (1995); (4) De Becker et al. (2006); (5) Rauw & De Becker (2004); (6) Mahy et al. (2009); (7) Sana et al. (2008); (8) Sana et al. (2009); (9) Kiminki et al. (2008); (10) Kiminki et al. (2009); (11) Kiminki et al. (2010)

^aUpper bound obtained from modeling complete fraction.

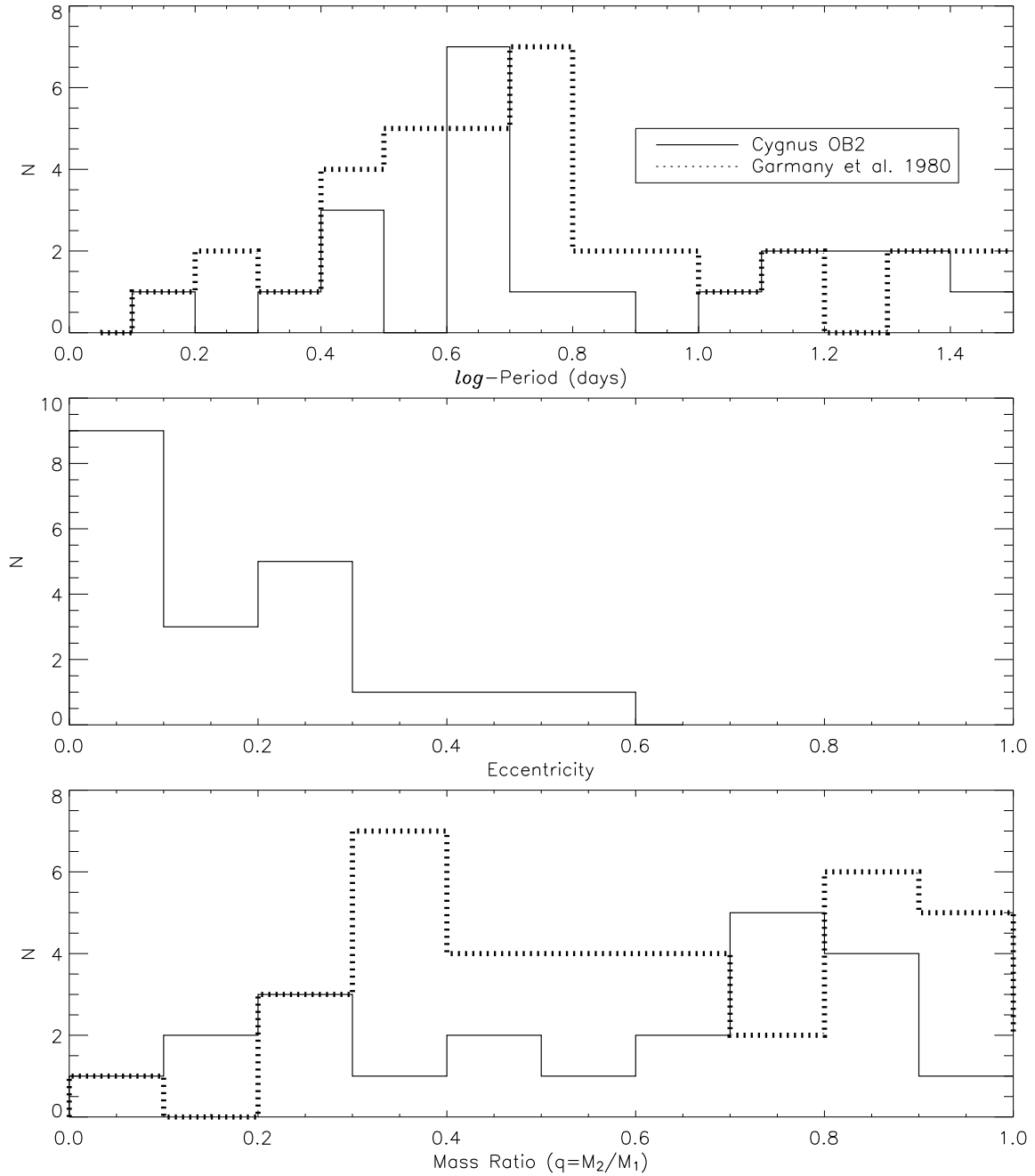


Fig. 1.— Histograms of the Cyg OB2 orbital period distribution in \log -Period (days) (top panel), orbital eccentricity distribution (middle panel), and mass ratio distribution (bottom panel). The orbital period and mass ratio distributions from Garmany et al. (1980) are illustrated by the dashed lines.

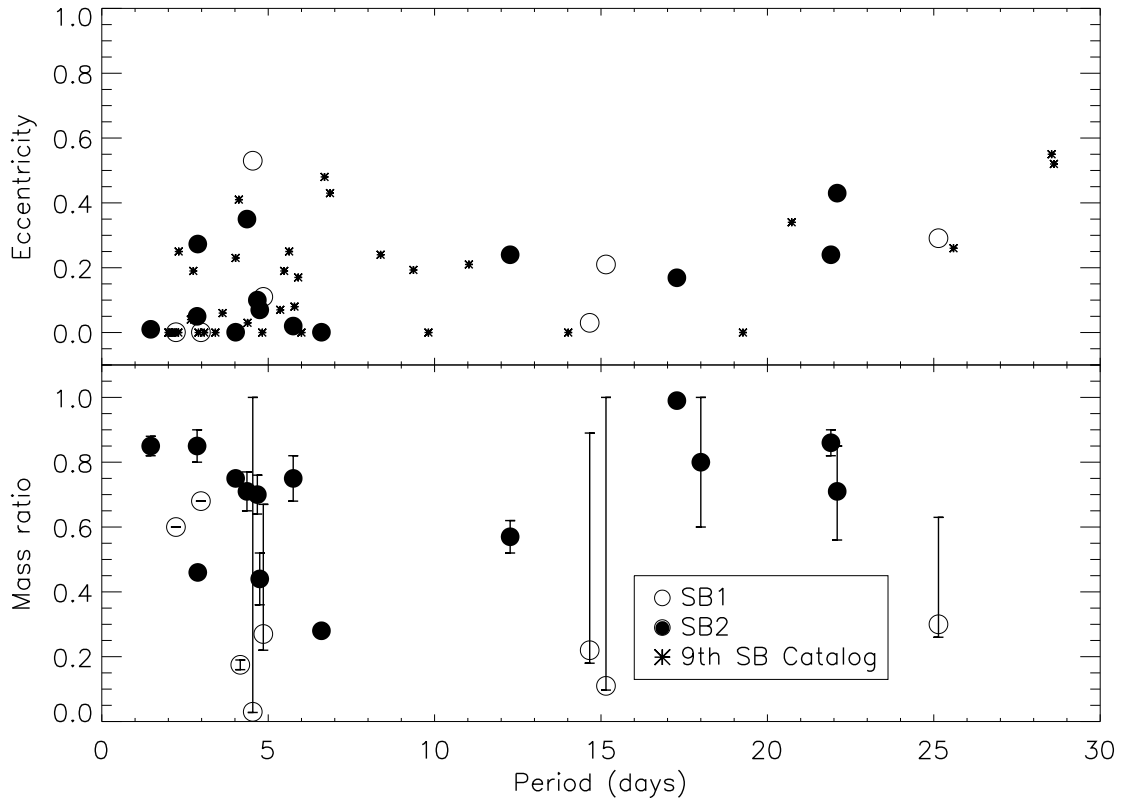


Fig. 2.— Eccentricity versus period (top panel) and mass ratio versus period (bottom panel) for 22 of the 24 known massive star binaries in Cyg OB2. SB1s are represented by open circles and SB2s are represented by filled circles. The data for massive star binaries of the Ninth Spectroscopic Binary Catalog (Pourbaix et al. 2004) are over-plotted for comparison (asterisks).

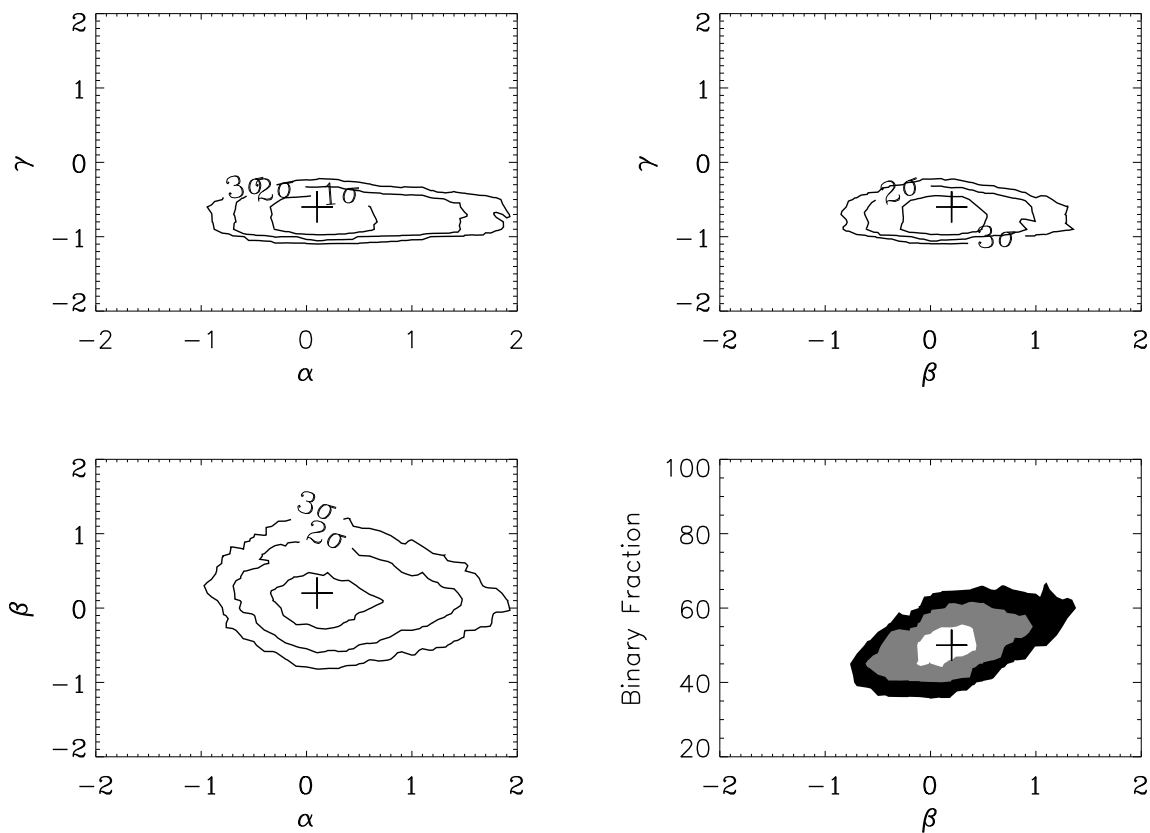


Fig. 3.— Contour plots depicting the probabilities of K–S tests between the observed orbital parameter and radial velocity data of the “complete” sample and the MC code fits. Contours in the upper left panel are for a $\beta = 0.2$ and $B.F. = 50\%$. Contours in the upper right panel are for a $\alpha = 0.1$ and $B.F. = 50\%$. Contours in the bottom left panel are for a $\gamma = -0.6$ and $B.F. = 50\%$. Contours in the bottom right panel are for a $\alpha = 0.1$ and $\gamma = -0.6$.

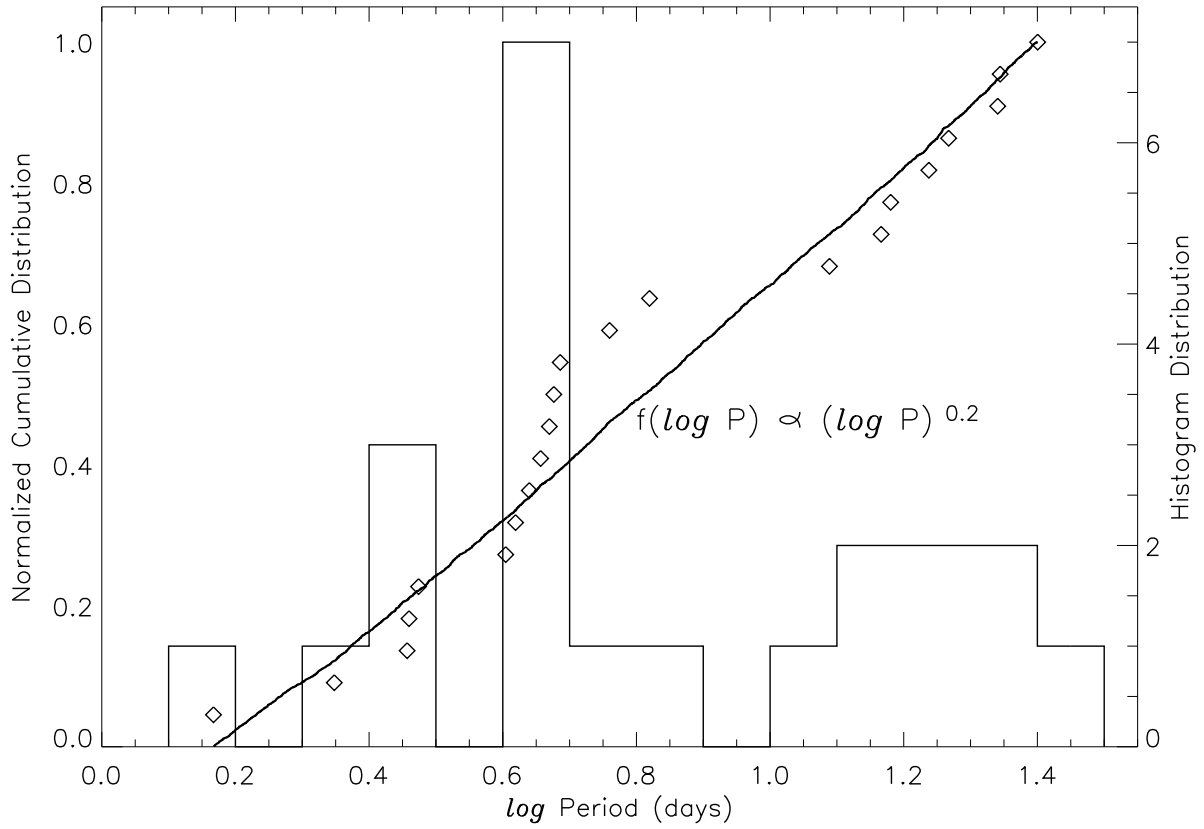


Fig. 4.— Cumulative period distribution (diamonds) and conventional histogram for the observed orbital periods. The solid curve is the cumulative period distribution for the best MC code fit ($\beta = 0.2$).

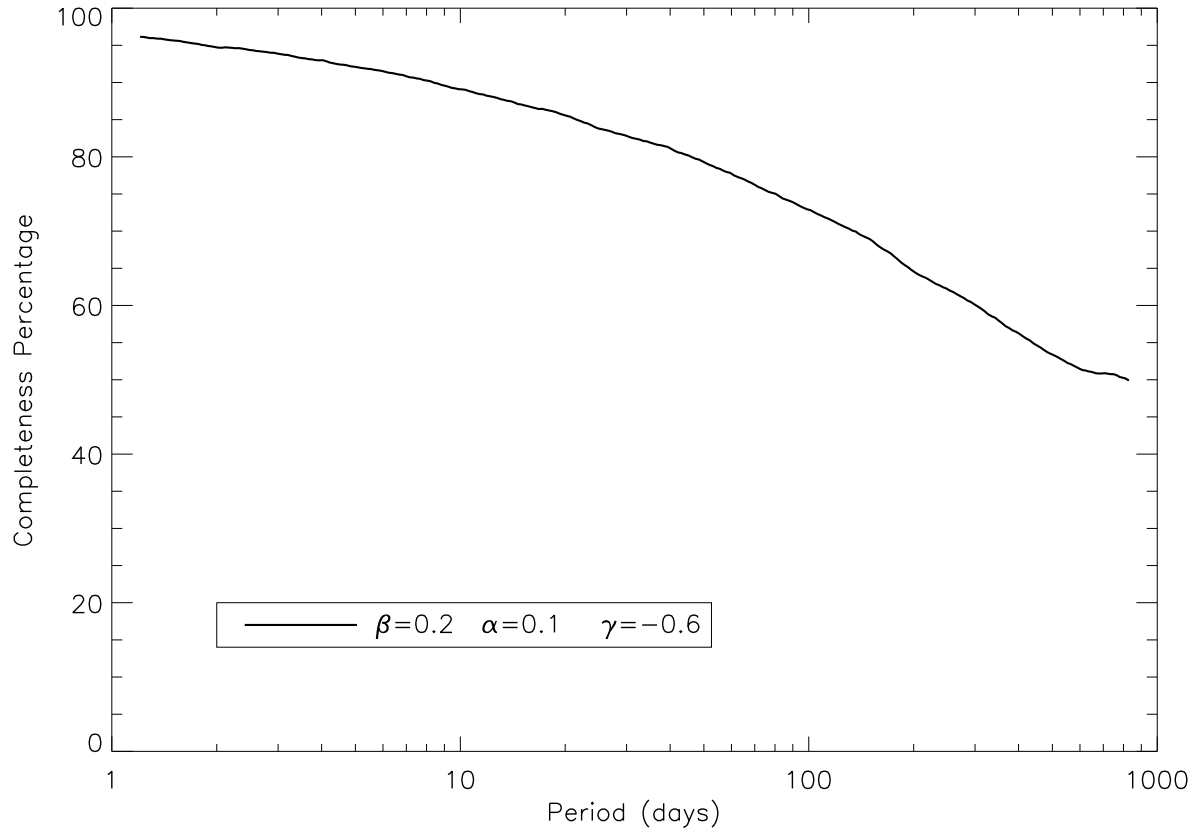


Fig. 5.— Survey completeness as a function of orbital period for the best-fit power-law indices.

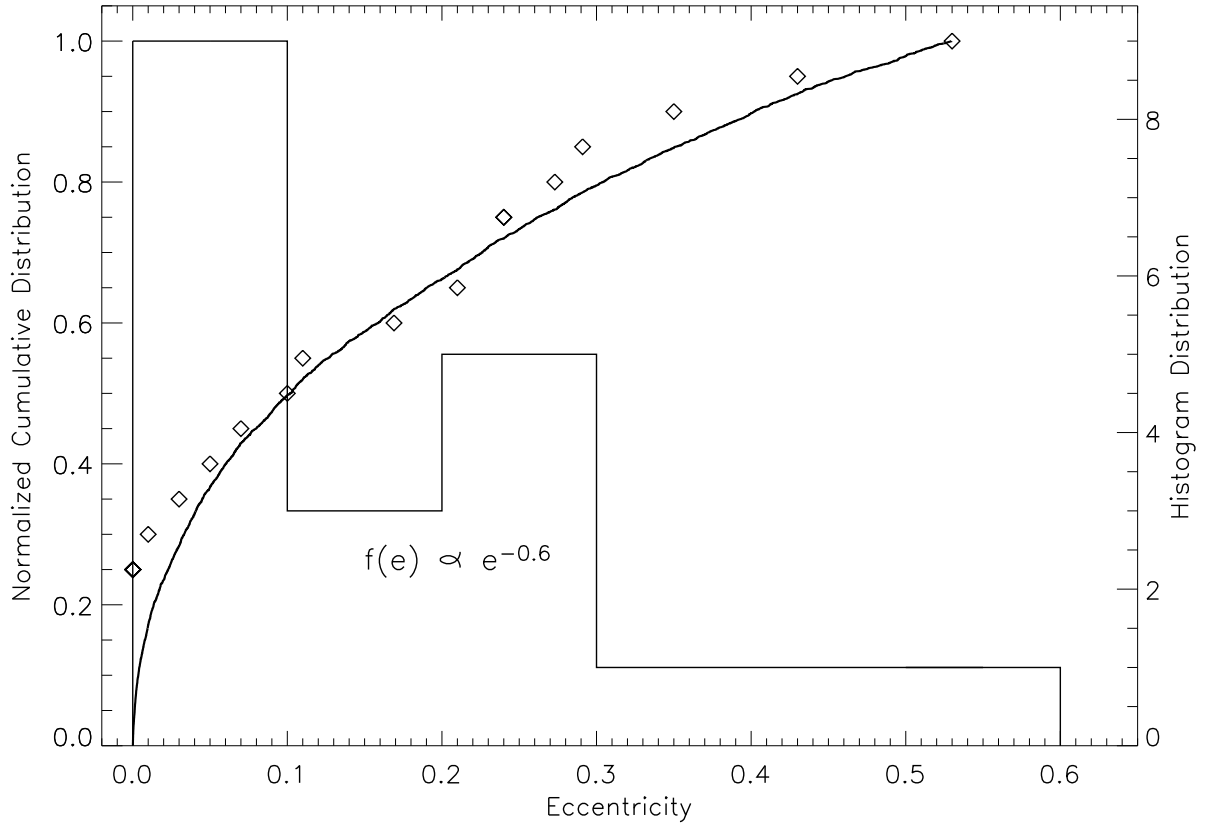


Fig. 6.— Normalized cumulative distribution (diamonds) and conventional histogram for the observed orbital eccentricities. The solid curve is the normalized cumulative distribution for the best MC code fit, $\gamma = -0.6$.

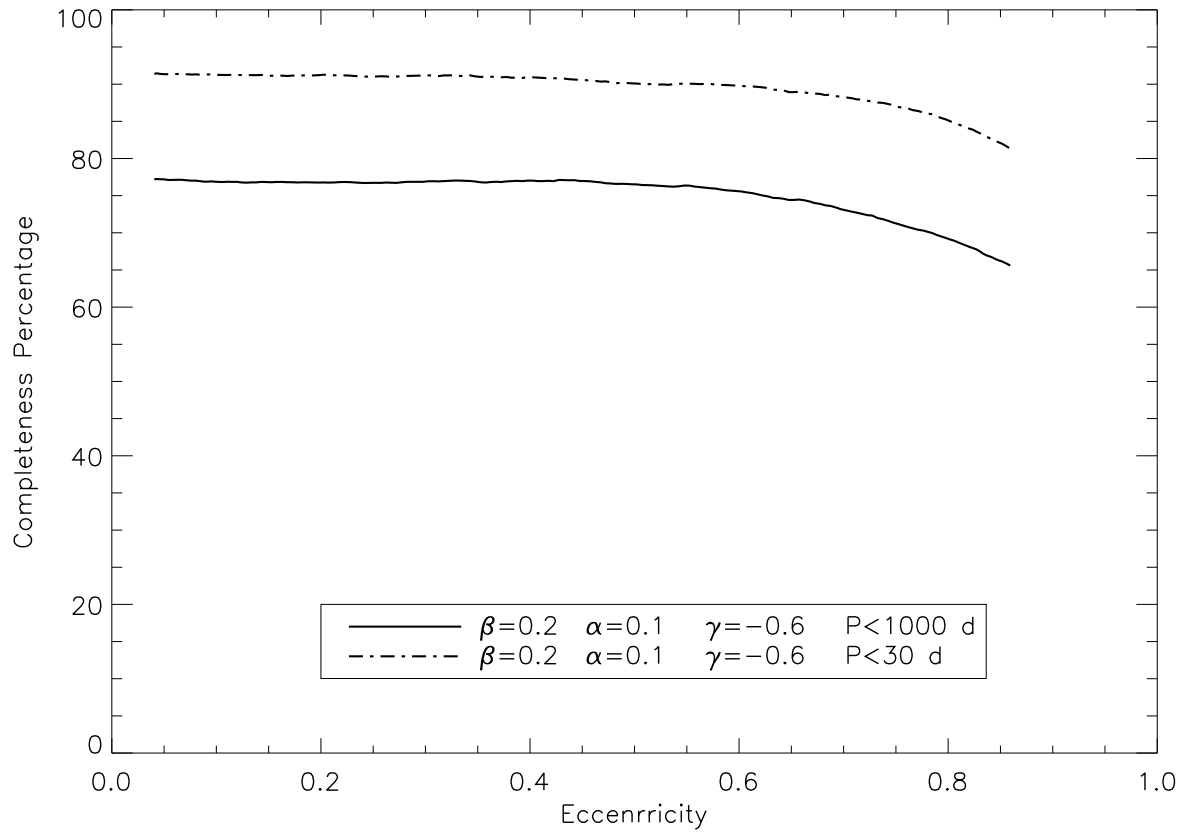


Fig. 7.— Survey completeness as a function of eccentricity for the best-fit power-law indices. The solid curve represents the period range of 1–1000 days and the dot-dash curve represents the period range of 1–30 days.

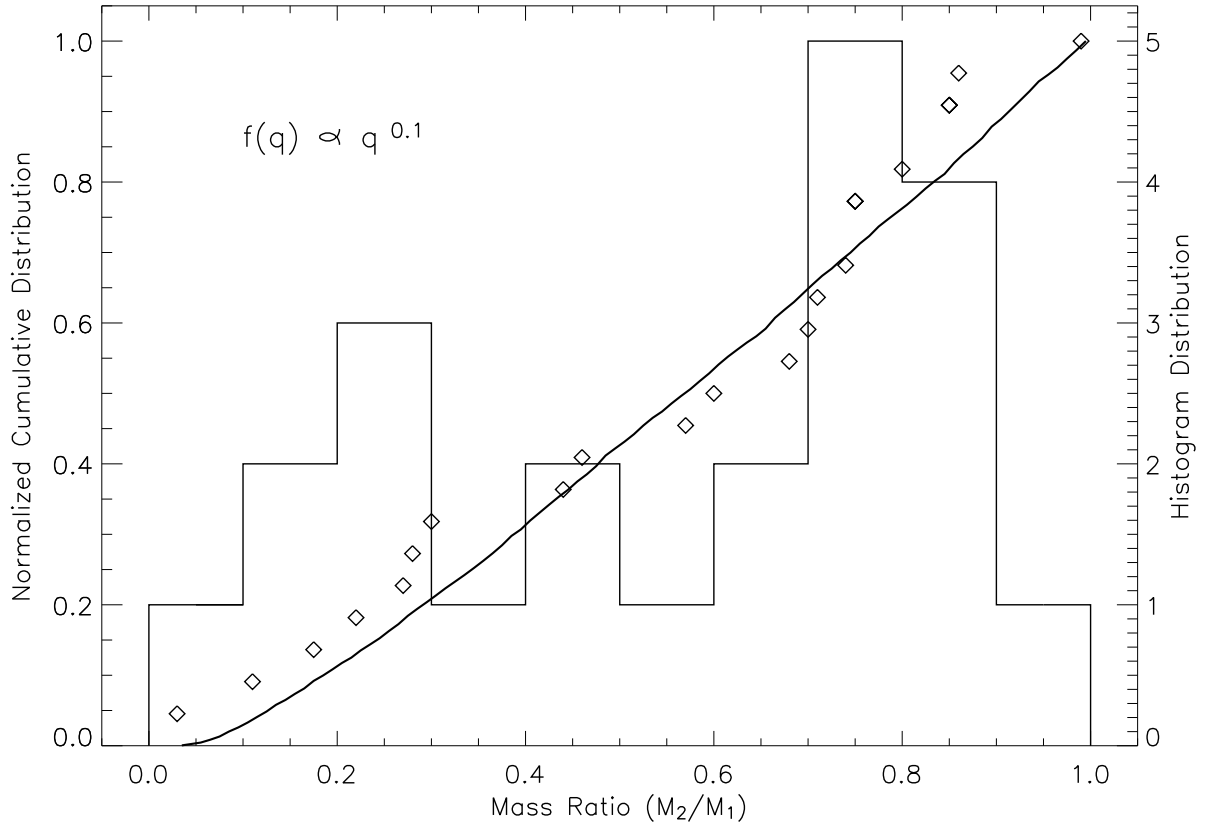


Fig. 8.— Normalized cumulative distribution (diamonds) and conventional histogram for the observed orbital mass ratios. The solid curve is the normalized cumulative distribution for the best MC code fit, $\alpha = 0.1$.

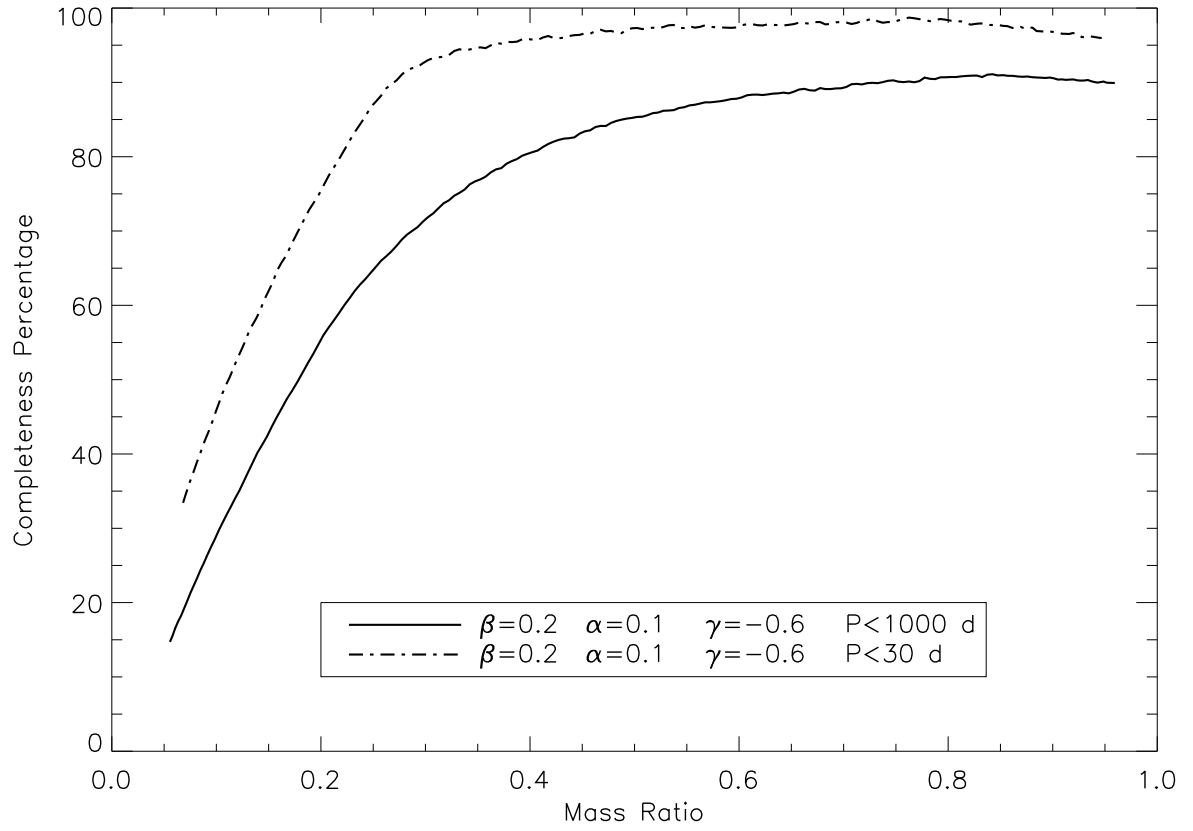


Fig. 9.— Survey completeness as a function of mass ratio for systems with periods $P < 30$ days (dot-dash curve) and $P < 1000$ days (solid curve) for the adopted best-fit power-law indices. .

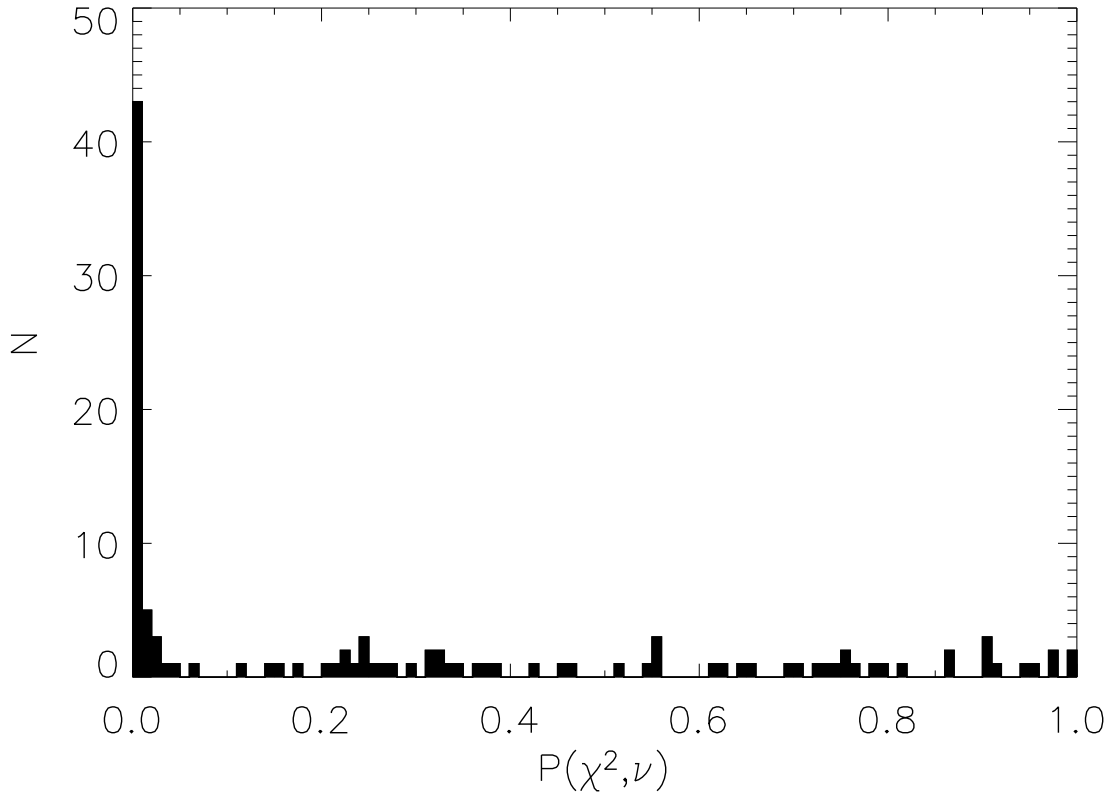


Fig. 10.— χ^2 probability density function for radial velocity measurements from the Cyg OB2 survey. Systems with $P(\chi^2, \nu) < 5\%$ are probable velocity variables.

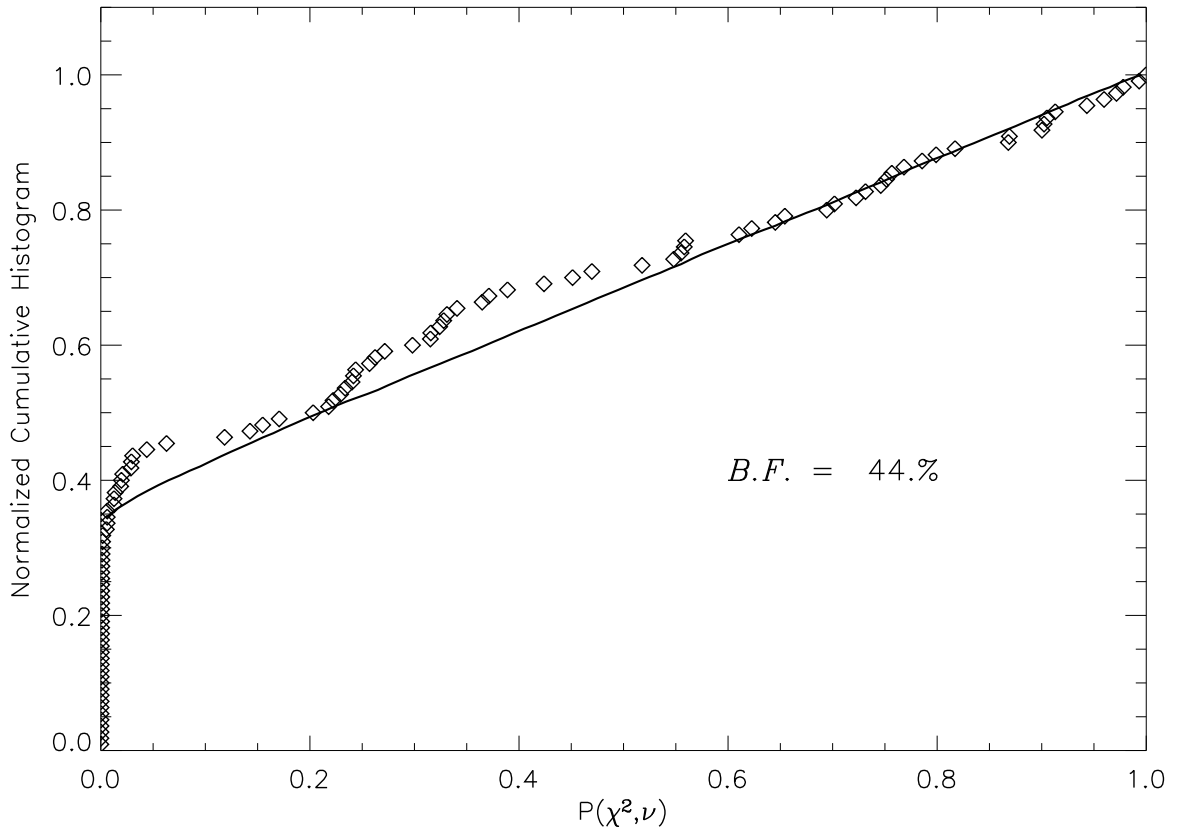


Fig. 11.— The cumulative distribution of χ^2 probabilities for the observed data (diamonds) and the best MC code fit (solid curve). The best fit represents a binary fraction of 44%.

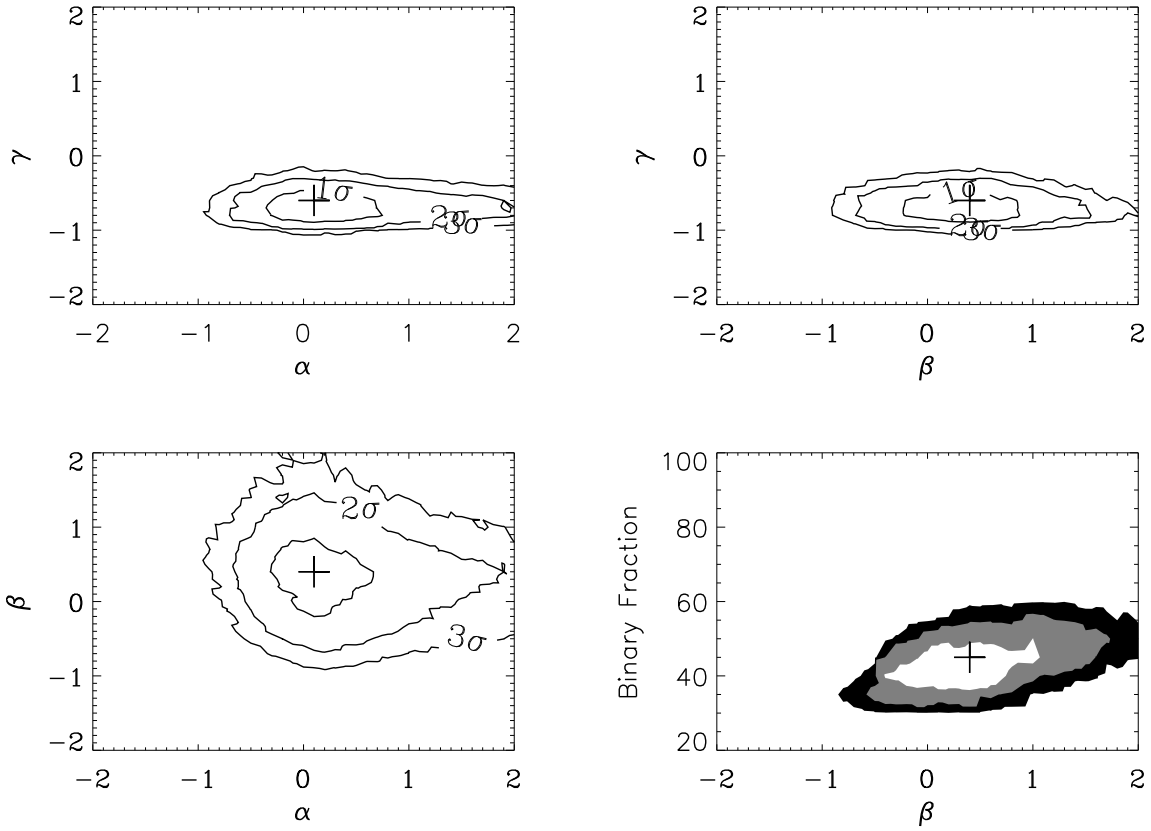


Fig. 12.— Contour plots depicting the probabilities of K–S tests as in Figure 3, but for the observed orbital parameter and radial velocity data of the “unbiased” sample and the MC code fits and with $B.F. = 44\%$.

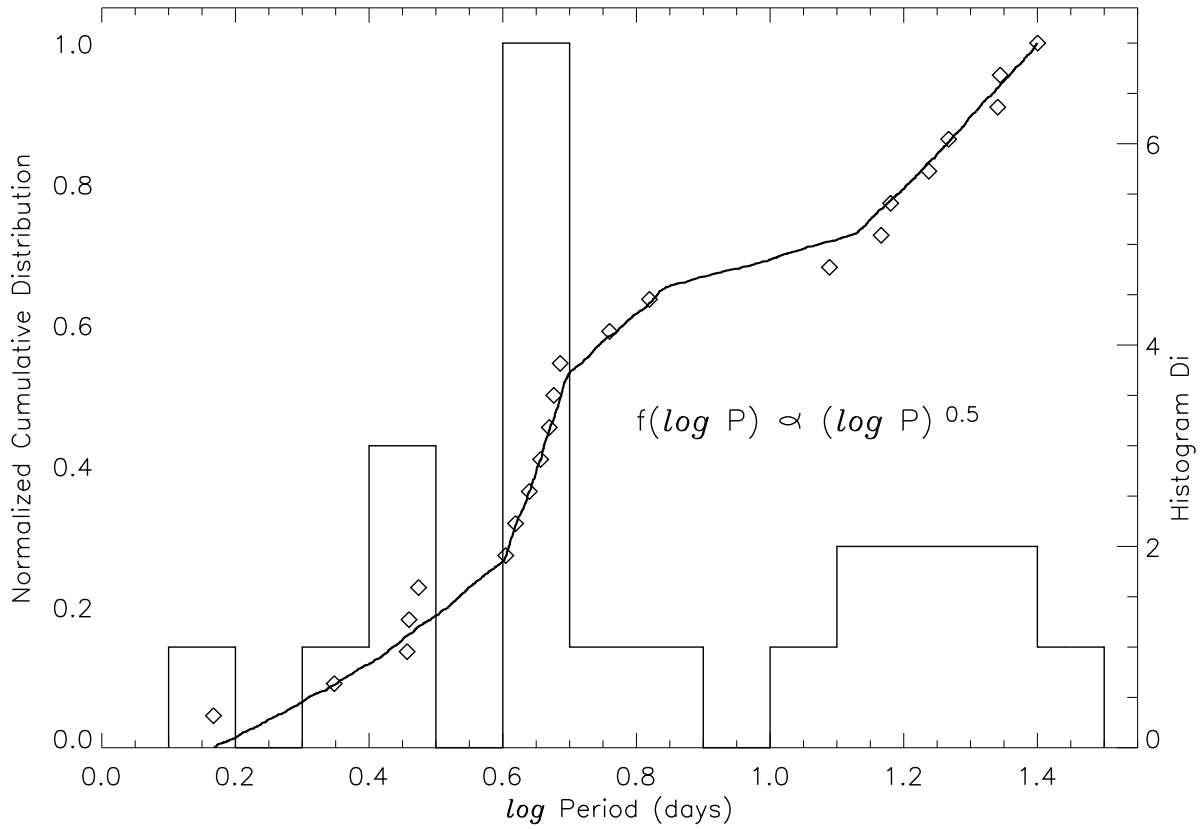


Fig. 13.— Normalized cumulative distribution (diamonds) and conventional histogram for the observed orbital periods. The solid curve is the cumulative distribution for the best MC code fit, assuming a 70% orbital period migration from $P=7\text{--}13.5$ days to $P=4\text{--}5$ days.

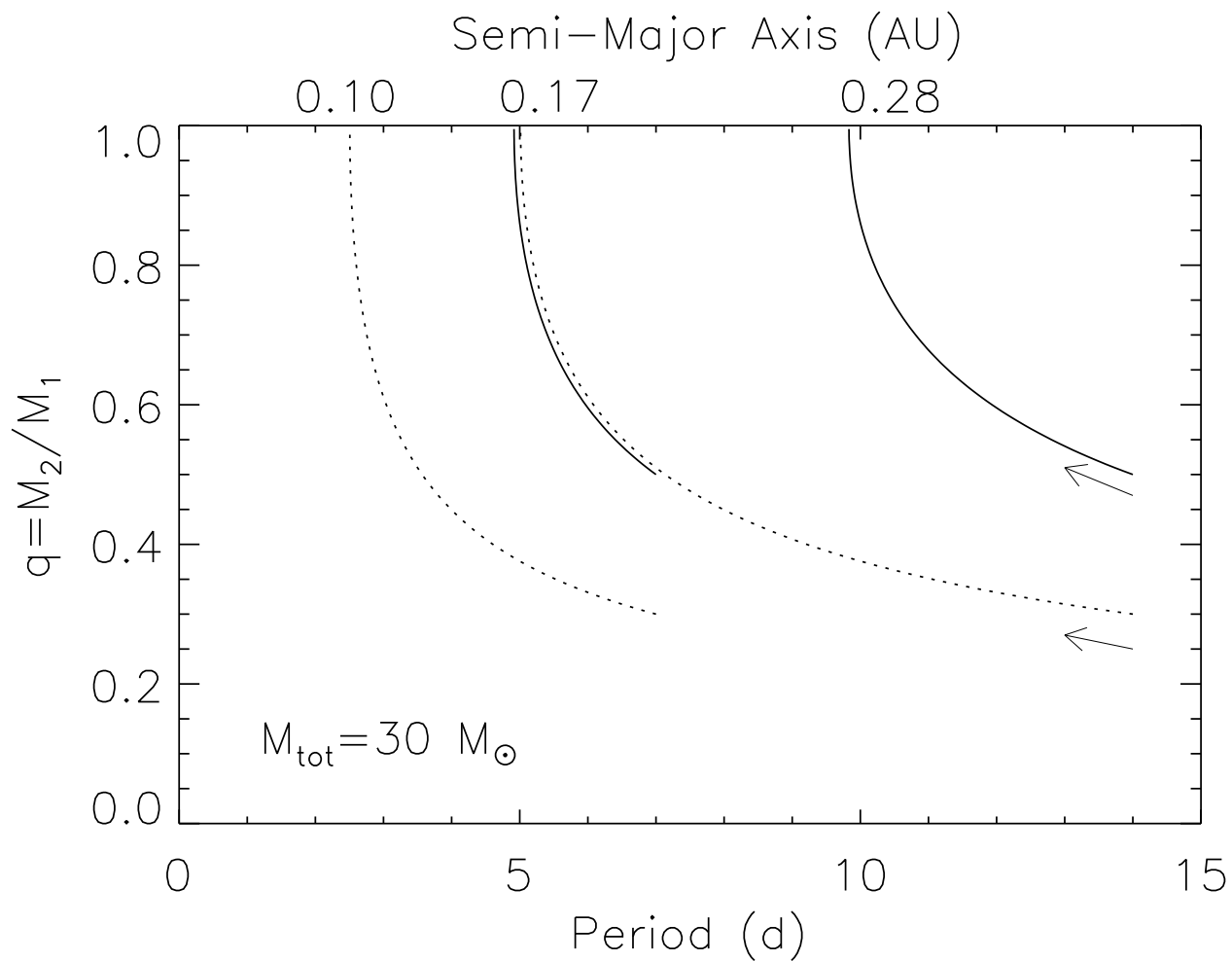


Fig. 14.— The evolution of orbital period/semi-major axis and mass ratio for a binary system with a total mass of $30 M_{\odot}$ as the primary loses mass to the secondary. Arrows show the direction of evolution as systems shift toward shorter periods (smaller orbits) and larger mass ratio. The solid and dotted tracks show the evolution of systems with different initial masses ratios and orbital periods. Systems with initial periods $P=7-14$ days and $q < 0.3$ end up as systems near 3–5 days and $q \sim 1$.